This is a preprint, the final version is subject to change, of the American Mineralogist (MSA)
Cite as Authors (Year) Title. American Mineralogist, in press.
(DOI will not work until issue is live.) DOI: http://dx.doi.org/10.2138/am-2016-5680

Revision 1

Carlsonite, $(NH_4)_5Fe^{3+}{}_3O(SO_4)_6 \cdot 7H_2O$, and huizingite-(Al), $(NH_4)_9Al_3(SO_4)_8(OH)_2 \cdot 4H_2O$, two new minerals from a natural fire in an oil-bearing shale near Milan, Ohio

ANTHONY R. KAMPF*[1], R. PETER RICHARDS[2], BARBARA P. NASH[3], JAMES B. MUROWCHICK[4], AND JOHN F. RAKOVAN[5]

[1]Mineral Sciences Department, Natural History Museum of Los Angeles County, 900 Exposition Boulevard, Los Angeles, CA 90007, U.S.A.
[2]Geology Department, Oberlin College, Oberlin, OH 44074, U.S.A.
[3]Department of Geology and Geophysics, University of Utah, Salt Lake City, Utah 84112, U.S.A.
[4]Department of Geosciences, University of Missouri-Kansas City, 420 Flarsheim Hall, 5110 Rockhill Road, Kansas City, MO 64110, U.S.A.
[5]Department of Geology and Environmental Earth Science, Miami University, Oxford, OH 45056, U.S.A.
*Email: akampf@nhm.org

ABSTRACT

The new minerals carlsonite (IMA2014-067), $(NH_4)_5Fe^{3+}{}_3O(SO_4)_6 \cdot 7H_2O$, and huizingite-(Al) (IMA2015-014), $(NH_4)_9Al_3(SO_4)_8(OH)_2 \cdot 4H_2O$, formed from a natural fire in an oil-bearing shale near Milan, Ohio. Carlsonite crystals are yellow to orange-brown thick tablets, flattened on {001}, or stout prisms, elongated on [110], up to about 0.5 mm in size. The mineral has a tan streak, vitreous luster, Mohs hardness of 2, brittle tenacity, irregular

fracture, perfect {001} cleavage, calculated density of 2.167 g·cm^{-3} and is easily soluble in H_2O. Carlsonite is optically biaxial (–), $\alpha = 1.576(1)$, $\beta = 1.585(1)$ and $\gamma = 1.591(1)$ (white light). Huizingite-(Al) crystals, typically intergrown in light greenish yellow drusy aggregates, are tabular to bladed, flattened on {100}, up to about 0.25 mm in maximum dimension. The mineral has a white streak, vitreous luster, Mohs hardness of 2½, brittle tenacity, irregular fracture, no cleavage, calculated density of 2.026 g·cm^{-3} and is easily soluble in H_2O. Huizingite-(Al) is optically biaxial (+) with $\alpha = 1.543(1)$, $\beta = 1.545(1)$ and $\gamma = 1.563(1)$ (589.6 nm light). Raman and infrared spectroscopy was conducted on both minerals. Electron microprobe analyses provided the empirical formulas $[(NH_4)_{4.64}Na_{0.24}K_{0.12}]_{\Sigma 5.00}Fe^{3+}_{3.05}O(SO_4)_6 \cdot 6.93H_2O$ and $[(NH_4)_{8.76}Na_{0.22}K_{0.02}]_{\Sigma 9.00}(Al_{1.65}Fe^{3+}_{1.34})_{\Sigma 2.99}(OH)_{1.98}(H_2O)_{4.02}(SO_4)_{8.00}$ for carlsonite and huizingite-(Al), respectively. Huizingite compositions with Fe>Al were noted. Carlsonite is triclinic, $P\bar{1}$, $a = 9.5927(2)$, $b = 9.7679(3)$ $c = 18.3995(13)$ Å, $\alpha = 93.250(7)°$, $\beta = 95.258(7)°$, $\gamma = 117.993(8)°$, $V = 1506.15(16)$ Å^3, and $Z = 2$. Huizingite-(Al) is triclinic, $P\bar{1}$, $a = 9.7093(3)$, $b = 10.4341(3)$, $c = 10.7027(8)$ Å, $\alpha = 77.231(5)°$, $\beta = 74.860(5)°$, $\gamma = 66.104(5)°$, $V = 948.73(9)$ Å^3, and $Z = 1$. The crystal structures of carlsonite ($R_1 = 0.030$) and huizingite ($R_1 = 0.040$) are bipartite, each consisting of a structural unit and an interstitial unit. For carlsonite, the structural unit is a $[Fe^{3+}_3O(H_2O)_3(SO_4)_6]^{5-}$ cluster and the interstitial complex is $[(NH_4)_5(H_2O)_4]^{5+}$. For huizingite-(Al), the structural unit is a $[(Al,Fe^{3+})_3(OH)_2(H_2O)_4(SO_4)_6]^{5-}$ cluster and the interstitial complex is $[(NH_4)_9(SO_4)_2]^{5+}$. In the carlsonite cluster, three FeO_6 octahedra share a common vertex, while in the huizingite-(Al) cluster, three $(Al,Fe)O_6$ octahedra form an abbreviated corner-linked chain. The cluster in carlsonite is the same as that in metavoltine, while the huizingite-(Al) cluster is unique. The range of Lewis basicity of the structural unit in carlsonite is 0.23–0.11 valence units (*vu*) and in huizingite-(Al) it is 0.20–0.12 *vu*; the corresponding Lewis acidities of the interstitial complexes in these

structures are 0.13 and 0.14 *vu*, respectively. A characteristic Lewis acid strength of 0.13 *vu* is suggested for NH_4^+ when it is in its most typical coordinations of 7 to 8. Carlsonite is named for the late Ernest H. Carlson (1933–2010), former Professor of Mineralogy at Kent State University. Huizingite is named for Terry E. Huizing (born 1938), Adjunct Curator of Mineralogy for the Cincinnati Museum Center, and Marie E. Huizing (born 1939), Editor of *Rocks & Minerals* since 1978.

Keywords: carlsonite; huizingite-(Al); new mineral; crystal structure; Raman spectroscopy; Infrared spectroscopy; Lewis acidity-basicity; Huron Shale burn site, Milan, Ohio.

INTRODUCTION

This paper reports the descriptions of the first two terrestrial (non-meteoritic) minerals to have been first discovered in the state of Ohio. These minerals, carlsonite and huizingite-(Al), formed as the result of a non-anthropogenic fire in an oil-bearing shale along the Huron River.

Carlsonite is named for Ernest H. Carlson (1933–2010). Dr. Carlson (Ph.D., McGill University, 1966) was professor of mineralogy at Kent State University in Kent, Ohio, from 1966 until his retirement in 2009. He was a Fellow of both the Society of Economic Geologists and the Association of Exploration Geochemists. Dr Carlson is perhaps best known for his studies of Ohio minerals and his authorship of Ohio Geological Survey Bulletin 69, *Minerals of Ohio* (1991). At the time of his death, Dr. Carlson was engaged in initial studies of the minerals of the Huron Shale burn site at which carlsonite and huizingite-(Al) were found, and he performed some of the early identifications of the minerals from this occurrence.

Huizingite is named for Terry E. Huizing (born 1938) and Marie E. Huizing (born 1939) of Cincinnati, Ohio. Terry has been an avid mineral collector since childhood. He and Marie met in college and married in 1961 following graduation, he with a B.S. in chemical engineering and she with a degree in secondary education with a major in English. Marie caught the mineral-collecting bug from Terry and both became (and still are) very active in the Cincinnati Mineral Society. Marie wrote and edited the society's newsletter, *The Quarry*, for more than 15 years. She was asked to assume the duties of Editor of *Rocks & Minerals* in 1978, a job that she has very effectively executed ever since, with Terry at her side serving as a Consulting Editor and helping with the promotion of the magazine. Terry has also served as North American representative for several other mineralogical publications, has published a number of mineralogical articles and, since the late 1970s, has served as the Adjunct Curator of Mineralogy for the Cincinnati Museum Center (formerly the Cincinnati Museum of Natural History). In recognition of these and many other contributions to the earth sciences, both Terry and Marie have received numerous honors. Terry received the Cincinnati Mineral Society Educational Foundation Award in 1984 and the American Federation Scholarship Foundation Award in 1991 for "distinguished achievement in the field of earth sciences". Marie received the Cincinnati Mineral Society Educational Foundation Award in 1978, the Carnegie Mineralogical Award for 1995 and the Mineralogical Society of America's Distinguished Public Service Award for 2007. Terry and Marie Huizing have agreed to the naming of this mineral in their honor. The -(Al) suffix is used to indicate that this mineral is the Al-dominant member of a series with its not-yet-described Fe-dominant counterpart, for which the name huizingite-(Fe) is proposed.

The new minerals and their names were approved by the Commission on New Minerals, Nomenclature and Classification of the International Mineralogical Association (carlsonite: IMA2014-067; huizingite-(Al): IMA2015-014). The carlsonite description is

based on one holotype and one cotype specimen, both of which are deposited in the collections of the Natural History Museum of Los Angeles County, catalogue numbers 65544 and 65545. The description of huizingite-(Al) is based on one holotype specimen, which is deposited in the collections of the Natural History Museum of Los Angeles County, catalogue number 65576.

OCCURRENCE

Carlsonite and huizingite-(Al) occur in a suite of minerals that resulted from a natural fire in an oil-bearing shale exposed at the interface between an eroded stream cliff (up to 7.5 m high) and its talus pile (~4.5 m thick) along the Huron River in north-central Ohio, approximately 6.1 km WSW of Milan, Ohio, U.S.A. (41°16'41.4"N, 82°40'27.0"W). The fire started in September of 2009, as the result of spontaneous combustion, and burned until March of 2011 (Figure 1). The occurrence is referred to as the Huron Shale burn site.

The rock unit exposed is the late Devonian Huron Shale member of the Ohio Shale formation, a dark grey to black marine, carbon-rich shale containing ironstone concretions, finely divided pyrite and pyrite nodules, and >10% organic matter. A sample taken from a four-meter cliff exposure near Milan, about six kilometers to the northeast of the fire site, yielded 5.2 gallons of oil per ton of shale (Hoover 1960). The geometry of the talus slope favors access of oxygen to pyrite, but also the sequestration of heat, which led to the spontaneous combustion. The fire was concentrated at the interface between talus slope and cliff, but burned away from the cliff into the talus pile in some areas. It burned to a depth of about 2 m. The mineral suite formed by sublimation and condensation on the surfaces of rocks within the talus pile as gases from the fire cooled (Figure 2). Surface temperatures at the vent were between 204°C and 260°C. A temperature probe operated by the Huron County Engineers Office registered a 426°C reading at a depth of half a meter. These temperatures

were measured during a moderately intense stage of the fire. The cliff and talus slope formed as the result of natural erosion; the fire occurred without any form of human intervention and was sustained naturally by the oil in the shale.

Minerals directly associated with carlsonite include anhydrite, boussingaultite, gypsum, and lonecreekite. Minerals directly associated with huizingite-(Al) include adranosite-(Al), anhydrite, boussingaultite, mascagnite, and salammoniac. Other minerals in the assemblage include adranosite-(Fe), alunogen, anhydrite, boussingaultite, clairite, ferrinatrite, gypsum, halotrichite, kremersite, letovicite, lonecreekite, mascagnite, metavoltine, pyracmonite, sabieite (2*H* and 3*R* polytypes; Kampf et al. 2014), salammoniac, sulfur, tschermigite, and voltaite.

Carlsonite and huizingite-(Al) are exceedingly rare minerals, thus far known only from a few specimens at a single occurrence, and neither has previously been reported as a synthetic phase. They formed at ambient pressure, but in an extreme and ephemeral environment characterized by a steep temperature gradient, indicating that they probably have very narrow stability ranges.

APPEARANCE AND PROPERTIES

Carlsonite

Carlsonite crystals are thick tablets, flattened on {001}, or stout prisms, elongated on [110], up to about 0.5 mm in size (Fig. 3). The crystals forms observed are {100}, {001}, {1-10}, {111}, (1-1-1} and {01-2} (Fig. 4). Cross-hatched twinning was rarely observed under crossed polars. Carlsonite is yellow to orange-brown, with a tan streak. Crystals are transparent with vitreous luster and display no fluorescence. The Mohs hardness based upon scratch tests is 2. Tenacity is brittle, fracture is irregular and cleavage is perfect on {001}. The density calculated based on the empirical formula using single-crystal unit-cell data is 2.167

150 g·cm^{-3}. Crystals are easily soluble in room temperature H_2O. The mineral is optically biaxial
151 (–) with indices of refraction $\alpha = 1.576(1)$, $\beta = 1.585(1)$, and $\gamma = 1.591(1)$ determined in white
152 light. The $2V$ measured directly using a spindle stage is 80(1)°. The calculated $2V$ is 78°.
153 Strong $r > v$ dispersion was observed. The incompletely determined optical orientation is X
154 $\approx\perp\{001\}$, $Z \approx [110]$. The pleochroism is X yellow, Y and Z orange; $X < Y \approx Z$. The Gladstone-
155 Dale compatibility index $1 - (K_P/K_C)$ is 0.001 for the empirical formula, in the range of
156 superior compatibility (Mandarino 2007).
157
158 **Huizingite-(Al)**
159 Huizingite-(Al) crystals are tabular, on {100}, to bladed, up to about 0.25 mm in
160 maximum dimension. Crystals are typically intergrown in drusy aggregates (Figs. 5 and 6).
161 The crystal forms observed are {100}, {010}, {001} and {110} (Fig. 7). No twinning was
162 observed. Huizingite-(Al) is light greenish yellow, with a white streak. Crystals are
163 transparent with vitreous luster and display no fluorescence. The Mohs hardness based upon
164 scratch tests is 2½. Tenacity is brittle, fracture is irregular and the mineral displays no
165 cleavage. The density calculated based on the empirical formula using single-crystal cell data
166 is 2.026 g·cm^{-3}. Crystals are easily soluble in room temperature H_2O. The mineral is optically
167 biaxial (+) with indices of refraction $\alpha = 1.543(1)$, $\beta = 1.545(1)$, $\gamma = 1.563(1)$ determined
168 using 589.6 nm light. The $2V$ measured directly using a spindle stage is 40(3)°. The calculated
169 $2V$ is 37°. Strong $r > v$ dispersion was observed. The optical orientation is $X \wedge \mathbf{a} = 24°$, $Y \wedge \mathbf{b} =$
170 25°, $Z \wedge \mathbf{c} = 27°$. The pleochroism is X pale yellow, Y and Z nearly colorless; $X > Y \approx Z$.
171 Crystals exhibit irregularly zoned extinction, apparently related to Al:Fe compositional
172 zonation. During conoscopic observation, the isogyres were quite diffuse, presumably due to
173 the combination of zoned optical properties and strong dispersion. The Gladstone-Dale

compatibility index $1 - (K_P/K_C)$ is -0.015 for the empirical formula, in the range of superior compatibility (Mandarino 2007).

RAMAN AND INFRARED SPECTROSCOPY

Raman analysis of single crystals of huizingite-(Al), within a 0.28 mm cluster of crystals, and a single crystal of carlsonite in a similar sized cluster were conducted with a Renishaw InVia Raman Microscope. The spectrometer interfaced to the microscope employed a 1800 groove/mm grating and a charge-coupled detector. The samples were excited using a HeNe laser (632 nm) that was focused onto the sample using a 20× (0.40 N.A.) objective for the huizingite and a 50× (0.85 N.A.) objective for carlsonite. The same objectives were employed to collect the back-scattered Raman radiation. The spectra were collected with a spectral resolution of 4 cm^{-1}, over the range of 100–4000 cm^{-1}, using an integration time of 120 s per scan, and samples in unknown orientations. The collected spectra were essentially featureless above 1600 cm^{-1}. Five individual scans were averaged to produce the final Raman spectrum (Figs. 8 and 9). Abscissa values were calibrated using the phonon band of single-crystal silicon located at 520.7 ± 0.3 wavenumber.

The huizingite spectrum was collected at full laser power (10.0 mW) with no harm to the sample. The following intense bands are observed at (centroid positions in cm^{-1}): 223, 263, 448, 468, 478, 618, 641, 673, 980, 1003, 1010, 1027, 1064, 1123, 1151 and 1205. Most of the observed bands in the Raman spectra relate to the four structurally distinct SO_4^{-2} groups. Based on comparison to other sulfate minerals the following (speculative) band assignments can be made: 1) The most intense bands 980, 1003, 1010, and 1027 cm^{-1} are from the symmetric stretch, ν_1, of the four sulfate groups; 2) bands 1064, 1123, 1151, and 1205 cm^{-1} are from the ν_3 modes of the sulfate groups; 3) bands in the 618-673 cm^{-1} region are from the ν_4 modes of the sulfate groups; 4) bands in the 448–478 cm^{-1} region are from the ν_2 modes of

199 the sulfate groups; and 5) bands at 223 and 263 cm^{-1} are uncertain but possibly due to $^{[VI]}$Fe-O
200 modes.

201 The carlsonite spectrum was collected at 10% laser power (1.0 mW) because the full
202 10 mW beam caused sample burning and the formation of hematite, for which a sharp Raman
203 spectrum was produced. After data collection, a 5 mW beam was used for further analysis and
204 did not affect the sample. The following intense bands are observed at (centroid positions in
205 cm^{-1}): 245, 275, 436, 487, 514, 552, 576, 617, 629, 670, 1015, 1066, 1104, 1140, 1160, 1188
206 and 1219. Band assignments are similar to those of huizingite-(Al).

207 Raman signals from structural ammonium and water, in the vicinity of 3300 cm^{-1},
208 were also investigated in both samples. For huizingite, there were no observable peaks in this
209 region. With the 10.0 mW beam, a very weak but discernible envelope of peaks was observed
210 around 3300 cm^{-1} in carlsonite; however, at lower powers these peaks were not detectable.

211 Although the presence of ammonium in huizingite was not detected in Raman and
212 only a weak broad signal was observed in carlsonite, FTIR clearly shows the presence of
213 ammonia in these two minerals. Attenuated total internal reflection (ATR) spectra were
214 collected with a Perkin-Elmer Spotlight 400 infrared microscope interfaced to a Perkin-Elmer
215 Spectrum One Fourier transform infrared spectrometer (FTIR). The system employed a 100 ×
216 100 μm, liquid nitrogen cooled, mercury cadmium telluride (HgCdTe) detector. The standard
217 drop-down germanium internal reflection element was employed in conjunction with a 50 ×
218 50 μm aperture. Each spectrum collected (Figs. 10 and 11) represents the average of 128
219 individual scans possessing a spectral resolution of 4 cm^{-1}.

220 The normal vibrational modes of unbound ammonium have frequencies of 3033 =
221 $\nu_1(A_1)$, 1680 = $\nu_2(E)$, 3137 = $\nu_3(F_2)$ and 1400 = $\nu_4(F_2)$ cm^{-1} (Nakamoto 1986). Of these only ν_3
222 and ν_4 are IR active; however, the lower symmetry sites of a crystal structure may allow the ν_1
223 and ν_2 modes to become active. The frequencies of these modes are also shifted as a result of

bonding effects in carlsonite and huizingite. FTIR spectra clearly show the presence of ammonium in these minerals by the 1416 and 1413 cm^{-1} bands, respectively. Other modes are observable but their IR absorptions can be difficult to distinguish from those of structural water. For example, the 3044 and 3022 cm^{-1} bands, in these minerals respectively, are likely the ν_1 mode in ammonium. The ammonium ν_3 mode appears at 3176 cm^{-1} in carlsonite and at 3192 cm^{-1} in huizingite. The band at 1667 cm^{-1} in huizingite is likely from the ammonium ν_2 vibrational mode but a band in this region for carlsonite is not observed. In carlsonite the weak band with a maximum at 1624 is most likely the bending mode of the water molecules. This feature is not observed in the huizingite, possibly due to the lower water concentration and broadening of the signal due to hydrogen bonding. Finally, the broad shoulder around 3500 cm^{-1} in carlsonite is likely from the OH stretching modes in water which may in part also contribute to the band associated with ammonium in the vicinity of 3300 cm^{-1} (Szakall et al. 2012). Thus, there is an absence of or weak contribution by typical H_2O absorptions, especially in the OH stretching region. Similar results were reported by Knop et al (1985) for $(NH_4)_2[AlF_5(H_2O)]$. They concluded that the OH stretching absorption in that phase underlies the group of peaks in the 3100–2900 cm^{-1} region that result from ammonium absorptions.

CHEMICAL COMPOSITION

Analyses of carlsonite (7 on six crystals) and huizingite-(Al) (10 on four crystals) were performed at the University of Utah on a Cameca SX-50 electron microprobe with four wavelength-dispersive spectrometers utilizing Probe for EPMA software (Probe Software, Inc.). A 15 KeV accelerating voltage and a 20 μm beam diameter were used for both minerals; a 20 nA beam current was used for carlsonite and a 10 nA beam current was used for huizingite-(Al). Counting times were 40 s for N and 20 s for other elements. Nitrogen was analyzed with a 60Å W/Si multilayer pseudocrystal (Cameca PC-1). The sample and nitrogen

249 standard (synthetic AlN) were carbon-coated at the same time to assure an equivalent
250 thickness of the carbon layer. Other standards employed are albite (Na), sanidine (K),
251 hematite (Fe) and celestine (S). Raw X-ray intensities were corrected for matrix effects with a
252 $\phi(\rho z)$ (PAP) algorithm (Pouchou and Pichoir 1991).

253 Electron microprobe analysis of low atomic number elements such as nitrogen is
254 complicated by a low cross-section for ionization and high absorption of the soft X-rays. Our
255 analyses confirmed the presence of significant N; however, our $(NH_4)_2O$ values are less than
256 those predicted by the structures (50% of predicted for carlsonite and 86% of predicted for
257 huizingite-(Al). The nature of the structure suggests that NH_4^+ is weakly bonded and some is
258 probably quickly lost, along with H_2O, under vacuum, either initially during carbon coating of
259 the sample or subsequently in the microprobe chamber. Monitoring of the N*K*α intensity
260 during each spot analysis showed only a slight decrease in N concentration with time under
261 the electron beam for which a correction was applied, but as noted above, it is likely that NH_3
262 was lost under vacuum prior to the analyses. Unfortunately, there is insufficient material for
263 direct determinations of N or H by CHN analysis. Consequently, the $(NH_4)_2O$ and H_2O
264 contents were calculated by stoichiometry based upon the crystal-structure determinations.
265 For carlsonite the high EPMA total after addition of calculated $(NH_4)_2O$ and H_2O is attributed
266 to the loss of these constituents under vacuum, which results in higher concentrations for the
267 remaining constituents. While the loss of $(NH_4)_2O$ and H_2O under vacuum should be expected
268 to provide a high EPMA total for huizingite as well, in fact the analytical total was low. We
269 attribute this to huizingite being very susceptible to beam damage, even when using low beam
270 current and a 20 μm diameter defocused beam. The results for carlsonite are presented in
271 Table 1a and those for huizingite in Table 1b.

272 The empirical formula for carlsonite (based on 6 S *apfu*) is
273 $[(NH_4)_{4.64}Na_{0.24}K_{0.12}]_{\Sigma 5.00}Fe^{3+}_{3.05}O(SO_4)_6 \cdot 6.93H_2O$. The simplified formula is

274 $(NH_4)_5Fe^{3+}{}_3O(SO_4)_6 \cdot 7H_2O$, which requires $(NH_4)_2O$ 13.34, Fe_2O_3 24.54, SO_3 49.21, H_2O
275 12.92, total 100%. The empirical formula for huizingite-(Al) (based on 38 O *apfu*) is
276 $[(NH_4)_{8.76}Na_{0.22}K_{0.02}]_{\Sigma 9.00}(Al_{1.65}Fe^{3+}{}_{1.34})_{\Sigma 2.99}(SO_4)_{8.00}(OH)_{1.98} \cdot 4.02H_2O$. The simplified end-
277 member formula is $(NH_4)_9Al_3(SO_4)_8(OH)_2 \cdot 4H_2O$, which for the Al end member requires
278 $(NH_4)_2O$ 20.96, Al_2O_3 13.68, SO_3 57.30, H_2O 8.06, total 100 wt%, and for the intermediate
279 member with Al:Fe = 1 requires $(NH_4)_2O$ 20.18, Al_2O_3 6.59, Fe_2O_3 10.31, SO_3 55.16, H_2O
280 7.76, total 100 wt%.

281 Among the 10 analyses of huizingite on which the results in Table 1b are based, the
282 Al:Fe ratio ranged from 0.86 to 2.03 or, in terms of the empirical formula, from $(Al_{1.39}Fe_{1.61})$
283 to $(Al_{2.03}Fe_{0.99})$. Both Al- and Fe-dominant regions were found in every crystal analyzed and
284 no spatial core-to-rim variation was found in a survey of Al and Fe contents over these and
285 additional crystals. Our findings indicate that, on average, the crystals are significantly higher
286 in Al than Fe and, in crystal regions where Fe is greater than Al, it is only slightly so. Of the
287 10 analyses included in Table 1, five are Al dominant (Al:Fe = 1.43–2.03) and five are Fe
288 dominant (Al:Fe = 0.86–0.97). Furthermore, Al significantly dominates over Fe (on average)
289 in the crystal used for the structure refinement $(Al_{1.72}Fe_{1.28})$. Because available material does
290 not allow the characterization of the Fe-dominant phase and the material characterized here is,
291 on average, Al dominant, we are describing only the Al-dominant phase. However, because
292 we have demonstrated the existence of the Fe-dominant phase, we recommend the use of a
293 suffix-based nomenclature for the end-members (Al- and Fe-dominant) of this series, i.e.
294 huizingite-(Al) and huizingite-(Fe).
295

296 ## X-RAY CRYSTALLOGRAPHY AND STRUCTURE DETERMINATION

297 Both powder and single-crystal X-ray diffraction studies were carried out using a
298 Rigaku R-Axis Rapid II curved imaging plate microdiffractometer, with monochromatized

299 Mo*Kα* radiation. For the powder-diffraction studies, a Gandolfi-like motion on the φ and ω
300 axes was used to randomize the sample. Observed *d* values and intensities were derived by
301 profile fitting using JADE 2010 software (Materials Data, Inc.). Data (in Å for Mo*K*α) are
302 given in Table 2 along with the calculated pattern.
303 The Rigaku CrystalClear software package was used for processing intensity data,
304 including the application of empirical multi-scan absorption corrections using ABSCOR
305 (Higashi, 2001). The structures were solved by direct methods using SIR2004 (Burla et al.
306 2005). SHELXL-2013 (Sheldrick 2008) was used for the refinements of the structures. For
307 both structures, the location of all non-hydrogen sites was straightforward. After refinement
308 of these sites with anisotropic displacement parameters, difference-Fourier maps provided the
309 locations of all H atom sites associated with the H_2O and NH_4 groups in carlsonite and the
310 OH, H_2O, and NH_4 groups in huizingite-(Al); however, the H sites associated with N5 in
311 huizingite-(Al) are disordered and partially occupied, as can be expected for a NH_4 group on a
312 center of symmetry (0,½,0). The H sites were refined using soft distance restraints with N–H
313 = 0.90(3), O–H = 0.82(3), H–H of NH_4 = 1.45(3) and H–H of H_2O = 1.30(3) Å. The H–H
314 restraint was not used for the disordered NH_4 group mentioned above. U_{eq} of each H was set
315 to 1.2 times that of the N or O atom to which it is bonded. The refinement of the huizingite
316 structure converged well with these restraints; however, the carlsonite refinement exhibited
317 relatively large shifts in the final refinement cycle: maximum shift/su = 1.323 and mean
318 shift/su = 0.036. The removal of the distance restraints allowed the refinement to converge
319 nicely (maximum shift/su = 0.002 and mean shift/su = 0.000); however, some of the resulting
320 N–H and O–H distances were significantly too high or too low. Consequently, we have
321 elected to report the refinement of the carlsonite structure using the aforementioned restraints.
322 Details of the sample, data collection, and structure refinement for each mineral are provided

in Table 3, final atom coordinates and displacement parameters in Table 4, selected bond distances in Table 5 and a bond-valence analysis in Table 6.

DISCUSSION OF THE STRUCTURES

Carlsonite

Carlsonite is a bipartite structure that consists of a structural unit and an interstitial complex, as elucidated by Schindler and Hawthorne (2001). The $[Fe^{3+}_3O(H_2O)_3(SO_4)_6]^{5-}$ cluster defines the structural unit. The interstitial complex, ideally $[(NH_4)_5(H_2O)_4]^{5+}$, balances the charge of the structural unit and links the structural units together. The atomic arrangement of carlsonite is depicted in Figure 12 and the structural unit is shown in Figure 13.

A polytypic relationship may exist between carlsonite and clairite, $(NH_4)_2Fe_3(SO_4)_4(OH)_3{\cdot}3H_2O$; however, clairite crystals are generally of too poor quality for definitive single-crystal study. Note that clairite is reported to be slowly soluble in H_2O (Martini 1983). Our examination of clairite crystals from the Huron Shale burn site confirmed them to be very slowly soluble, requiring several hours to dissolve. By contrast, carlsonite crystals are easily soluble in H_2O, arguing against a simple polytypic relationship between the species.

The $[Fe^{3+}_3O(H_2O)_3(SO_4)_6]^{5-}$ cluster in the structure of carlsonite (Figure 6) is identical to that found in the structure of metavoltine, $Na_6K_2Fe^{2+}Fe^{3+}_6O_2(SO_4)_{12}{\cdot}18H_2O$ (Giacovazzo et al. 1976). In fact, the structures of carlsonite and metavoltine are remarkably similar, as shown in Figure 5. Note that the placements of the NH_4 groups in the structure of carlsonite are similar to the placements of Na and K in the structure of metavoltine, providing further support for our assignments of the NH_4 sites. The same cluster is also found in the structure of

347 Maus' salt, $K_5Fe^{3+}_3(SO_4)_6(OH)_2{\cdot}nH_2O$, and several related compounds (cf. Scordari et al.
348 1994).
349
350 **Huizingite-(Al)**
351 Huizingite-(Al) is also a bipartite structure. The $[(Al,Fe^{3+})_3(OH)_2(H_2O)_4(SO_4)_6]^{5-}$
352 cluster defines the structural unit and the interstitial complex has the formula
353 $[(NH_4)_9(SO_4)_2]^{5+}$. The atomic arrangement of huizingite-(Al) is depicted in Figure 14 and the
354 structural unit is compared to that of carlsonite in Figure 13.
355 The structural unit in the structure of huizingite-Al is a cluster containing the same
356 polyhedral components, three $M^{3+}O_6$ octahedra (M^{3+} = Fe or Al) and six SO_4 groups, that
357 make up the cluster in the structure of carlsonite; however, the polyhedra are linked quite
358 differently. In the carlsonite cluster, three FeO_6 octahedra share a common vertex, while in the
359 huizingite-(Al) cluster, three $(Al,Fe)O_6$ octahedra form an abbreviated corner-linked chain.
360 The polyhedral cluster in the huizingite-(Al) structure is unique, but has the same topology as
361 a segment of the $[Fe^{3+}(SO_4)_3]^{3-}$ polyhedral chain in the structure of sideronatrite (Scordari and
362 Ventruti 2009).
363
364 **NH_4–O bonding**
365 The NH_4–O bond lengths in the structure of carlsonite vary from 2.796 to 3.380 Å,
366 corresponding to coordinations of 7, 6, 8, 7, and 8 for $NH_4$1, $NH_4$2, $NH_4$3, $NH_4$4, and $NH_4$5,
367 respectively. Those in huizingite-(Al) vary from 2.729 to 3.281 Å, corresponding to
368 coordinations of 7, 7, 7, 8, and 6 for $NH_4$1, $NH_4$2, $NH_4$3, $NH_4$4, and $NH_4$5, respectively.
369 Khan and Baur (1972) surveyed NH_4-containing structures and noted that NH_4–O
370 coordinations vary from 4 to 9; for small (4 or 5) coordinations, the NH_4 group behaves more
371 like a conventional hydrogen-bond donor, forming nearly linear N–H···O bonds; for higher

372 coordinations, the NH_4 group behaves more like an alkali cation, with either the NH_4 group
373 exhibiting orientational disorder or the H bonds being polyfurcated. In a study of the crystal
374 structure of hannayite, $Mg_3(NH_4)_2(HPO_4)_4{\cdot}8H_2O$, Catti and Franchini-Angels (1976)
375 described the hybrid (or dual) bonding behavior of the NH_4^+ group between an ordered
376 hydrogen-bond donor and a strongly electropositive large alkali-like cation. They observed
377 that this dual behavior for NH_4^+ is apparently quite common. The dual-bonding behavior of
378 NH_4 is clearly observed in the structures of carlsonite and huizingite-(Al) (Table 5); with the
379 exceptions of HN5a in carlsonite and HN3d in huizingite-(Al), each of the H atoms associated
380 with the NH_4 groups forms a single short, nearly linear hydrogen bond to an O atom, while
381 other NH_4–O bonds are more appropriately regarded as electrostatic in nature. It is
382 noteworthy that the dual-bonding behavior of NH_4 was also reported in pyracmonite,
383 $(NH_4)_3Fe^{3+}(SO_4)_3$ (Demartin *et al*., 2010), a mineral that is also found in the Huron River burn
384 site mineral suite.
385
386 **Lewis acidity-basicity**
387 Hawthorne and Schindler (2008) noted that the strengths of the relatively weak bonds
388 between the strongly bonded *structural unit* (SU) and the *interstitial complex* (IC) usually
389 control the stability of a structure. Furthermore, they pointed out that the interaction between
390 the typically anionic SU and the typically cationic IC can be examined using the Principle of
391 Correspondence of Lewis acidity-basicity. The Lewis basicity (LB) of the SU reflects its
392 capacity to donate electron density and the Lewis acidity (LA) of the IC reflects its capacity to
393 accept electron density; these quantities are essentially equivalent to bond valence and are
394 expressed in valence units (*vu*). The Principle of Correspondence states that, when the LA
395 closely matches the LB, a stable structure will form.

Using the approach detailed by Hawthorne and Schindler (2008), the characteristic range in LB for the SU in carlsonite can be calculated as follows: The effective charge (EC) = the formal charge of the SU less the charge transferred by hydrogen bonding (6 H-bonds) = 5^- – $6 \times 0.2 = 6.2^-$. The charge deficiency per anion (CDA) = EC per O atom (28 O atoms) = $6.2^- / 28 = 0.22^-$. The range in the average number of bonds ($<NB_{in}>$) from the IC to O atoms in the SU obtained from Figure 8c in Hawthorne and Schindler (2008) $<NB_{in}> = 0.95–1.95$. The range in total number of bonds (RB) to the SU = $<NB_{in}> \times$ number of O atoms = (0.95–1.95) × 28 = 26.6–54.46. The range in LB of the SU of carlsonite = EC / RB = 6.2 / (26.6–54.46) = 0.23–0.11 *vu*. For huizingite-(Al), the same procedure was used; however, it is worth noting that the unconnected SO_4 group, included as part of the IC, must be considered as part of the SU for the purpose of computing the LB because of the unconnected SO_4 group's strong internal bonding. The resulting range in LB for the SU in huizingite-(Al) was calculated to be 0.20–0.12 *vu*.

Previous studies of Lewis acidity have largely overlooked the NH_4^+ group. In fact, prior listings of Lewis acid strengths for cations (cf. Hawthorne and Schindler 2008; Hawthorne 2012) do not include the NH_4^+ group. For purposes of calculating the LA of the IC in NH_4 phases, the distinction between hydrogen bonds and electrostatic bonds, discussed earlier, does not seem pertinent and the NH_4^+ group is probably best treated as a normal cation. The LA of the IC in carlsonite and huizingite-(Al) is computed as the formal charge of an NH_4^+ group (+1) divided by the average number of bonds emanating from each of the NH_4^+ groups, modified by any transformer H_2O groups. [For an explanation of transformer H_2O groups, the reader is referred to Hawthorne and Schindler (2008)]. The calculated LA of the IC in carlsonite is 0.13 *vu* and in huizingite-(Al) is 0.14 *vu*. In both cases, the principle of correspondence of Lewis acidity-basicity holds. Furthermore, the fact that in both cases the

match occurs at the lower range of Lewis basicity is an indication that the environment in which these phases formed was not highly acidic.

Finally, it is worth considering the typical or average value of Lewis acid strength that should be attributed to the NH_4^+ cation, in general. The 0.13–0.14 *vu* values noted above for carlsonite and huizingite-(Al) correspond to average coordination numbers (CN) in the 7 to 8 range. It is well known that NH_4^+ forms many oxysalts that are isostructural with corresponding K^+ salts (*cf*. Khan and Baur, 1972). The most common CN for K^+ is 8, which corresponds to a Lewis acid strength of 0.125 *vu*. Indeed, Brown (1981) provided a Lewis acid strength of 0.13 *vu* for K^+ and this has been used by subsequent workers. Consequently, we suggest that 0.13 *vu* be used as the characteristic Lewis acid strength for NH_4^+, in most cases (7 to 8 CN); however, this value is probably not appropriate for those structures in which NH_4^+ has small (4 or 5) CN. For example, NH_4^+ has an average CN of 4 in $(NH_4)_3PO_4{\cdot}3H_2O$ (Mootz and Wunderlich 1970), with each of three distinct NH_4^+ groups forming four hydrogen bonds to O atoms of PO_4^{3-} groups (which constitute the structural unit). The PO_4^{3-} oxyanion has a characteristic Lewis basicity of 0.25 *vu* (*cf*. Hawthorne and Schindler, 2008). In this structure, and others in which NH_4^+ has a CN of 4, it seems more appropriate to assign it a Lewis acid strength of 0.25 *vu* (charge/CN).

Relation of the structures to paragenesis

In a series of papers, Scordari and coworkers examined the structures and stabilities of some hydrated alkali iron sulfates (see Scordari et al. 1994, and references therein). These featured, in particular, phases containing the same $[Fe^{3+}{}_3O(H_2O)_3(SO_4)_6]^{5-}$ cluster that is found in carlsonite and metavoltine. They showed that these compounds gradually alter through dehydration to form phases with the ferrinatrite, $Na_3Fe(SO_4)_3{\cdot}3H_2O$, structure and that the transformation involves the rearrangement of the $[Fe^{3+}{}_3O(H_2O)_3(SO_4)_6]^{5-}$ clusters into

chains of composition $[Fe^{3+}(SO_4)_3]^{3-}$. Compounds containing Na^+, K^+, and H_3O^+ were examined; however, phases containing NH_4^+ were not considered. Interestingly, as noted above, the huizingite-(Al) cluster is essentially a segment of a sideronatrite polyhedral chain.

IMPLICATIONS

The close structural relationship between carlsonite and metavoltine is intriguing considering that metavoltine is a rather widely distributed mineral occurring as an alteration product of pyrite in arid climates, as a fumarolic sublimate and solfataric precipitate, as a post-mining product, and as a coal-fire sublimate. The last of these modes of occurrence, whether of natural or anthropogenic origin, is rather similar to that at the Huron River burn site. Ammonium-bearing phases are typical of coal-fire occurrences [*e.g.* the burning coal dumps of the Upper Silesian Coal Basin (Parafiniuk and Kruszewski 2009) and the burning Anna I coal mine dump, Alsdorf, Germany (Witzke et al. 2015)] and can occur, as well, in other types of deposits; yet an ammonium analogue of metavoltine has not been reported, either as a natural or synthetic phase; although Wendlandt and Harrison (2006) did report a NH_4-bearing metavoltine as a precipitate associated with uranium mill tailings disposal cells at the White Mesa Mill in Utah. It seems remarkable that the new mineral carlsonite has not previously been reported from other NH_4 mineral occurrences and particularly from those in which these phases have formed by sublimation from high-temperature gases. There are sufficient similarities in the powder X-ray diffraction patterns of carlsonite and metavoltine to suspect that carlsonite may have been mistaken for metavoltine in some previous studies of NH_4-rich mineral assemblages.

The new heteropolyhedral cluster in the structure of huizingite-(Al) is of interest simply because of its uniqueness, but more so because of insight that its existence may provide into the structural and paragenetic relations among the various hydrated ferric sulfate

minerals. In particular, it may exist as a complex in aqueous solutions or in solid-state transformations involving the formation and/or breakdown of sideronatrite-style $[Fe^{3+}(SO_4)_3]^{3-}$ chains. The fact that it has thus far only been found in a rare phase formed under extreme and very ephemeral conditions suggests that it has a very narrow stability range and its existence is normally transitory.

ACKNOWLEDGEMENTS

Uwe Kolitsch and an anonymous reviewer provided constructive comments on the manuscript. Frank Hawthorne is thanked for suggestions regarding the discussion of Lewis acidity-basicity. Will Shewfelt is acknowledged for bringing this mineral occurrence to the attention of the scientific community via the late Ernest Carlson of Kent State University. Ernest Carlson, Lance Kearns of John Madison University and George Robinson of the A.E. Seaman Mineralogical Museum (Michigan Technological University) are acknowledged for initial studies on the minerals from this occurrence. We are grateful to Dr. Andy Sommer of Miami University for use of his Raman and FTIR instruments and help with FTIR data collection. The electron microprobe laboratory at the University of Utah is supported in part by the National Science Foundation, the College of Mines and Earth Sciences, and the Department of Geology and Geophysics. Wil Mace of that department is acknowledged for assistance with the microprobe analyses. The SEM/EDS laboratory at Oberlin College, which provided initial recognition of most of the phases at the burn site, is partly supported by the National Science Foundation. A portion of this investigation was funded by the John Jago Trelawney Endowment to the Mineral Sciences Department of the Natural History Museum of Los Angeles County

REFERENCES

Brese, N.E., and O'Keeffe, M. (1991) Bond-valence parameters for solids. Acta Crystallographica, B47, 192–197.

Brown, I.D. (1981) The bond-valence method: an empirical approach to chemical structure and bonding. In: Structure and Bonding in Crystals Vol. 2 (eds. M. O'Keeffe, A. Navrotsky), pp. 1–30. Academic Press, New York 1981.

Brown, I.D., and Altermatt, D. (1985) Bond-valence parameters from a systematic analysis of the inorganic crystal structure database. Acta Crystallographica, B41, 244–247.

Burla, M.C., Caliandro, R., Camalli, M., Carrozzini, B., Cascarano, G.L., De Caro, L., Giacovazzo, C., Polidori, G., and Spagna, R. (2005) SIR2004: an improved tool for crystal structure determination and refinement. Journal of Applied Crystallography, 38, 381–388.

Catti, M., and Franchini-Angela, M. (1976) Hydrogen bonding in the crystalline state. Structure of $Mg_3(NH_4)_2(HPO_4)_4{\cdot}8H_2O$ (hannayite), and crystal-chemical relationships with schertelite and struvite. Acta Crystallographica, B32, 2842–2848.

Demartin, F., Gramaccioli, C.M., and Campostrini, I. (2010) Pyracmonite, $(NH_4)_3Fe(SO_4)_3$, a new ammonium iron sulfate from La Fossa Crater, Vulcano, Aeolian Islands, Italy. Canadian Mineralogist, 48, 307–313.

García-Rodríguez, L., Rute-Pérez, Á., Piñero, J.R., and González-Silgo, C. (2000) Bond-valence parameters for ammonium-anion interactions. Acta Crystallographica, B56, 565–569.

Giacovazzo, C., Scordari, F., Todisco, A., and Menchetti, S. (1976) Crystal structure model for metavoltine from Sierra Gorda. Tschermaks Mineralogische und Petrographische Mitteilungen, 23, 155–166.

Hawthorne, F.C. (2012) A bond-topological approach to theoretical mineralogy: crystal structure, chemical composition and chemical reactions. Physics and Chemistry of Minerals, 39, 841–874.

520 Hawthorne, F.C., and Schindler, M. (2008) Understanding the weakly bonded constituents in
521 oxysalt minerals. Zeitschrift für Kristallographie, 223, 41–68.
522 Higashi, T. (2001) ABSCOR. Rigaku Corporation, Tokyo.
523 Hoover, K.V. 1960. Devonian-Mississippian shale sequence in Ohio. Ohio Division of
524 Geological Survey, Informational Circular 27, 154 p.
525 Kampf, A.R., Richards, R.P., and Nash, B.P. (2014) The 2*H* and 3*R* polytypes of sabieite,
526 $NH_4Fe^{3+}(SO_4)_2$, from a natural fire in an oil-bearing shale near Milan, Ohio. American
527 Mineralogist, 98, 1500–1506.
528 Khan, A.A., and Baur, W.H. (1972) Salt hydrates. VIII. The crystal structures of sodium
529 ammonium orthochromate dihydrate and magnesium diammonium bis(hydrogen
530 orthophosphate) tetrahydrate and a discussion of the ammonium ion. Acta
531 Crystallographica, B28, 683–693.
532 Knop, O., Cameron, T.S., Deraniyagala, S.P., Adhikesavalu, D. , and Falk, M. (1985)
533 Infrared spectra of the ammonium ion in crystals. Part XIII. Crystal structure of
534 $(NH_4)_2[AlF_5(H_2O)]$ and NH_3D^+ probe-ion spectra in $(NH_4)_2[AlF_5(H_2O)]$, NH_4AlF_4, and
535 $(NH_4)_3ZnCl_5$, with remarks on structural filiation of AMF_4 fluorides. Canadian Journal of
536 Chemistry, 63, 516–525.
537 Mandarino, J.A. (2007) The Gladstone–Dale compatibility of minerals and its use in selecting
538 mineral species for further study. Canadian Mineralogist, 45, 1307–1324.
539 Martini, J.E.J. (1983) Lonecreekite, sabieite, and clairite, new secondary ammonium ferric-
540 iron sulfates from Lone Creek Fall cave, near Sabie, eastern Transvaal. Annals of the
541 Geological Survey of South Africa, 17, 29–34.
542 Mootz, V.-D. and Wunderlich, H. (1970) Die Kristallstustur von $(NH_4)_3PO_4 \cdot 3H_2O$,
543 Triammonium-orthophosphat-trihydrat. Acta Crystallographica, B26, 1826–1835 (in
544 German).

Nakamoto, K. (1986) Infrared and Raman Spectra of Inorganic and Coordination Compounds. Wiley and Sons, New York.

Parafiniuk, J., and Kruszewski, L. (2009) Ammonium minerals from burning coal-dumps of the Upper Silesian Coal Basin (Poland), Geological Quarterly, 53, 341–356.

Pouchou, J.-L., and Pichoir, F. (1991) Quantitative analysis of homogeneous or stratified microvolumes applying the model "PAP." In: K.F.J. Heinrich and D.E. Newbury (eds) Electron Probe Quantitation. Plenum Press, New York, pp. 3l–75.

Schindler, M., and Hawthorne, F.C. (2001) A bond-valence approach to the structure, chemistry, and paragenesis of hydroxyl-hydrated oxysalt minerals. I. Theory. Canadian Mineralogist, 39, 1225–1242.

Scordari, F., and Ventruti, G. (2009) Sideronatrite, $Na_2Fe(SO_4)_2(OH)\cdot 3H_2O$: Crystal structure of the orthorhombic polytype and OD character analysis. American Mineralogist, 94, 1679–1686.

Scordari, F., Stasi, F., Schingaro, E., and Comunale, G. (1994) A survey of $(Na,H_3O^+,K)_5Fe_3O(SO_4)_6\cdot H_2O$ compounds: architectural principles and influence of the Na–K replacement on their structures. Crystal structure, solid-state transformation and its relationship to some analogues. Zeitschrift für Kristallographie, 209, 733–737.

Sheldrick, G.M. (2008) A short history of SHELX. Acta Crystallographica, A64, 112–122.

Szakall, S., Sajo, I., Feher, B. and Bigi, S. (2012) Ammoniomagnesiovoltaite, a new voltaite-related mineral species from Pécs-Vasas, Hungary. The Canadian Mineralogist, 50, 65–72.

Wendlandt, R.F., and Harrison, W.J. (2006) Ammonium sulfate evaporites associated with uranium mill tailings disposal cells. American Geophysical Union, Fall Meeting 2006, abstract #V31D-0603.

569 Witzke, T., de Wit, F., Kolitsch, U., and Blaß, G. (2015) Mineralogy of the burning Anna I
570 coal mine dump, Alsdorf, Germany. p. 203-240, Chapter 7 in: Stracher, G.B., Prakash, A.
571 and Sokol, E.V.: Coal and Peat Fires: A Global Perspective, Volume 3: Case studies –
572 coal fires. Elsevier, 786 pp.

573

574 FIGURE CAPTIONS

575 Figure 1. Huron Shale burn site along the Huron River near Milan, Ohio, in early 2011.

576

577 Figure 2. Recently formed minerals near the interface between the cliff face and talus slope.

578 The white dendritic crystals are salammoniac. (FOV = 22 cm).

579

580 Figure 3. Carlsonite crystal. (FOV = 1 mm).

581

582 Figure 4. Crystal drawing of carlsonite tablet; clinographic projection in standard orientation.

583

584 Figure 5. Drusy intergrowths of huizingite-(Al) crystals with anhydrite. (FOV = 2.2 mm

585 across).

586

587 Figure 6. Huizingite-(Al) crystals on anhydrite. (FOV = 0.6 mm across).

588

589 Figure 7. Crystal drawing of huizingite-(Al) tablet; clinographic projection in standard

590 orientation.

591

592 Figure 8. Raman spectrum of carlsonite.

593

594 Figure 9. Raman spectrum of huizingite-(Al).

595

596 Figure 10. FTIR spectrum of carlsonite.

597

598 Figure 11. FTIR spectrum of huizingite-(Al).

599

600 Figure 12. Atomic arrangements of carlsonite and metavoltine, viewed down [100]. $Fe^{3+}O_6$
601 octahedra are orange, $Fe^{2+}O_6$ octahedra are green, SO_4 tetrahedra are yellow, K atoms are
602 light blue spheres, Na atoms are dark blue spheres, N atoms are red spheres, O atoms of
603 isolated H_2O groups are large white spheres and H atoms are small white spheres. N–H and
604 O–H bonds are shown as sticks. Unit cells are shown with dashed lines.

605

606 Figure 13. The structural units in carlsonite and huizingite-(Al). $Fe^{3+}O_6$ and AlO_6 octahedra
607 are orange, SO_4 tetrahedra are yellow.

608

609 Figure 14. Atomic arrangement of huizingite-(Al) viewed down [100]. The structural
610 components are as described in figures 12 and 13. Note that the disordered $NH_4$5 group on the
611 center of symmetry at (0,½,0).

612

613

614 Table 1a. Electron microprobe analytical results for carlsonite.

Const.	wt%	Range	SD	Normalized
$(NH_4)_2O$	6.30	6.03–6.48	0.15	
$(NH_4)_2O$*	12.75			12.30
Na_2O	0.79	0.42 – 1.13	0.24	0.76
K_2O	0.59	0.47 – 0.72	0.09	0.57
Fe_2O_3	25.70	25.17 – 26.42	0.51	24.79
SO_3	50.67	49.87 – 51.73	0.79	48.88
H_2O*	13.16			12.70
Total	103.66			100.00

615

616 Table 1b. Electron microprobe analytical results for huizingite-(Al).

Const.	wt%	Range	SD	Normalized
$(NH_4)_2O$	15.88	14.71 – 17.27	0.85	
$(NH_4)_2O$*	18.57			19.70
Na_2O	0.55	0.30 – 1.05	0.27	0.58
K_2O	0.09	0.06 – 0.12	0.02	0.10
Al_2O_3	6.85	5.53 – 8.59	1.20	7.27
Fe_2O_3	8.71	6.40 – 10.17	1.36	9.24
SO_3	52.14	49.91 – 53.66	1.11	55.32
H_2O*	7.35			7.80
Total	94.26			100.00

617 * based upon the crystal structure determination.

618

Table 2a. Powder X-ray diffraction data for carlsonite.*

I_{obs}	d_{obs}	d_{calc}	I_{calc}	$h\ k\ l$
100	9.23	9.1020	100	0 0 2
		8.5695	4	0 1 0
40	8.26	8.3939	25	1 0 0
		8.2936	7	-1 1 0
		8.1161	22	0-1 1
		8.0439	6	-1 0 1
43	7.57	7.6129	13	-1 1 1
		7.4831	17	1-1 1
		7.4353	22	0 1 1
		7.2612	4	1 0 1
8	6.67	6.6296	9	-1 0 2
		6.2011	2	-1 1 2
4	5.83	5.7953	4	1 0 2
5	5.28	5.2642	2	-1 0 3
		5.2403	4	0-1 3
23	4.93	4.9453	11	-1-1 1
		4.8726	11	-1 2 0
		4.8448	3	1-1 3
10	4.74	4.7757	9	-2 1 0
		4.7682	2	1-2 1
		4.7069	2	0 1 3
		4.3937	2	-2 1 2
8	4.302	4.2847	4	0 2 0
		4.2153	5	-2 0 1
8	4.136	4.1468	3	-2 2 0
		4.1305	2	-1-1 3
		4.0814	2	2-1 2
		4.0580	2	0-2 2
		4.0234	2	2-2 1
6	3.957	3.9746	2	2 0 1
		3.8978	6	1-2 3
14	3.726	3.7080	10	-1 2 3
		3.7036	2	0-2 3
13	3.597	3.5996	2	2-1 3
		3.5836	12	1 1 3
		3.5168	3	-1 0 5
9	3.441	3.4524	7	-2 1 4
		3.4141	3	1-2 4
		3.3879	3	2-2 3
20	3.328	3.3269	2	0 2 3
		3.3148	17	-2 0 4
		3.3061	2	1-1 5
		3.2693	4	-1-2 1
15	3.246	3.2536	5	2 0 3
		3.2443	8	-1 2 4
		3.2409	3	1 2 0
41	3.144	3.1566	27	2-1 4
		3.1382	4	-3 1 0
		3.1332	4	2-3 1
		3.1280	3	1 1 4
		3.1176	8	1 2 1
		3.1074	3	-2 3 1
		3.1006	4	-2 2 4
16	3.035	3.0717	8	-3 1 2
		3.0376	4	-1-2 3
		3.0289	7	-2 1 5
		3.0142	3	2-3 2
		2.9907	5	1-2 5
12	2.943	2.9687	4	-2 3 2
		2.9590	3	-1 3 2
		2.9285	3	1 2 2
		2.9203	4	-3 1 3
		2.8997	2	2 1 2
		2.8944	3	3-2 2
10	2.849	2.8476	6	-1 2 5
		2.8363	2	2-3 3
		2.8303	3	-1-2 4
5	2.758	2.7799	3	-2 3 3
		2.7465	3	1 1 5
		2.7237	2	1-3 4
		2.7055	2	2-2 5
6	2.666	2.6823	3	2 1 3
		2.6713	2	3-1 3
		2.6592	3	-3 2 4
		2.6311	2	0 2 5
		2.6286	2	3-3 2
7	2.463	2.4668	6	2 2 0
		2.4312	3	2-4 1
6	2.389	2.4010	3	-1-3 1
		2.3878	2	-4 2 0
		2.3621	3	-4 2 2
		2.3534	2	0 2 6
10	2.332	2.3442	3	0-2 7
		2.3245	3	-4 1 1
		2.3226	2	-1-3 3
		2.3165	3	-3 4 0
		2.2947	2	-3 4 1
8	2.268	2.2755	3	0 0 8
		2.2525	3	3 0 4
		2.2388	2	-3 4 2
5	2.210	2.2263	2	-3 3 5
		2.2085	2	0-3 6
		2.1938	2	4-3 2
2	2.128	2.1402	2	0-4 2
		2.1254	2	1 0 8
4	1.9225	1.9354	1	3-2 7
		1.9277	1	-3 5 0
		1.9241	1	3-5 1
		1.9195	1	4-2 5
		1.9179	1	2 2 5
5	1.8628	1.8706	2	1-5 1
		1.8623	2	-4-1 1
8	1.8216	1.8204	4	0 0 10
		1.8039	2	-5 4 1

*Calculated lines with $I < 2$ are omitted except those needed to index the observed line at 1.9225 Å.

Table 2b. Powder X-ray diffraction data for huizingite-(Al).*

I_{obs}	d_{obs}	d_{calc}	I_{calc}	$h\,k\,l$
30	10.33	10.2428	45	0 0 1
		9.4581	16	0 1 0
60	8.82	8.7110	79	1 0 0
11	8.07	8.0581	39	1 1 0
26	7.47	7.4504	8	0 1 1
		7.3731	44	1 0 1
28	6.55	6.5364	59	0-1 1
5	6.14	6.0830	17	-1 0 1
32	5.60	5.5952	47	-1-1 1
		5.4788	16	-1 1 0
69	5.037	5.1214	20	0 0 2
		5.0312	9	1 1 2
		5.0122	66	1 2 1
		4.9251	10	1-1 1
32	4.776	4.8408	15	1 0 2
		4.7573	24	2 1 1
		4.7423	7	-1 1 1
		4.7290	22	0 2 0
25	4.521	4.5242	45	0 2 1
22	4.337	4.3555	11	2 0 0
		4.3187	20	2 0 1
		4.2759	7	0-1 2
41	4.122	4.1844	10	2 2 1
		4.1276	14	1 2 2
		4.1094	5	-1-2 1
		4.0949	18	0-2 1
		4.0847	32	-1 0 2
		4.0290	2	2 2 0
		3.8477	3	-1-1 2
10	3.831	3.8292	16	1-1 2
		3.7252	2	0 2 2
		3.6866	2	2 0 2
		3.6593	2	-1 1 2
		3.6320	4	-1 2 0
38	3.534	3.5321	58	1 1 3
		3.4493	3	1 3 1
		3.4449	19	-1 2 1
		3.4269	100	-2-2 1
100	3.427	3.4219	6	2-1 1
		3.4143	7	0 0 3
		3.4018	2	1-2 1
		3.3919	14	1 3 0
		3.3543	33	0 1 3
		3.2898	17	2 3 1
		3.2682	2	0-2 2
		3.2167	12	1 2 3
		3.2140	3	3 1 1
68	3.204	3.2063	56	-2 1 1
		3.1979	12	2 1 3
		3.1689	2	2 3 0
		3.1585	7	1 3 2
		3.1527	31	0 3 0
		3.1172	4	3 1 0
		3.0967	11	2 3 2
		3.0854	5	0-1 3
		3.0813	3	2 2 3
94	3.043	3.0420	76	2-1 2
		3.0310	9	-1-3 1
		3.0184	43	3 1 2
		3.0010	8	3 2 2
		2.9800	2	2 0 3
		2.9586	7	1-1 3
		2.9464	5	3 0 1
		2.9350	2	1-2 2
		2.8605	4	-1-1 3
5	2.840	2.8564	6	0 3 2
		2.8049	5	3 3 1
		2.7976	5	-2-2 2
9	2.772	2.7646	10	3 0 2
		2.7545	2	-2 1 2
		2.7250	3	3 3 2
		2.7194	7	2 3 3
		2.7166	7	1 3 3
20	2.697	2.6973	5	-3-2 1
		2.6860	7	3 3 0
		2.6769	5	2-2 1
		2.6664	2	-1 3 0
		2.6623	2	-3 0 1
		2.6558	2	3 1 3
		2.6111	3	0-2 3
9	2.571	2.5764	13	1 4 1
		2.5574	2	0 1 4
		2.5410	2	-1-2 3
		2.5324	4	3-1 1
8	2.521	2.5129	10	-1 2 3
		2.4664	2	-2 0 3
18	2.458	2.4626	9	2-2 2
		2.4563	12	-2-1 3
		2.4313	4	-3-3 1
		2.4204	2	2 0 4
		2.4090	4	-3-1 2
		2.3941	3	0-1 4
		2.3860	2	0 2 4
		2.3728	2	0 4 1
11	2.369	2.3645	4	0 4 0
		2.3614	6	1-1 4
		2.3515	3	-1-4 1
		2.3289	3	-3-2 2
		2.3225	3	-2 1 3
12	2.316	2.3167	3	1-3 2
		2.3096	5	2 4 3
		2.3053	3	4 3 1
		2.2953	2	1 3 4
5	2.212	2.2108	5	3 4 3
		2.1857	2	2-2 3
10	2.175	2.1735	8	3-1 3
		2.1560	3	-1 3 3
		2.1512	2	-4-2 1
11	2.138	2.1379	10	-3-3 2
		2.1367	3	3-2 1
		2.1128	3	-1 2 4
		2.0949	8	-1 4 0
16	2.087	2.0922	2	4 4 2
		2.0861	8	2 2 5
		2.0734	2	1-2 4
		2.0601	2	-3-1 3
		2.0562	12	2 5 2
		2.0513	2	-4 0 1
15	2.048	2.0474	2	0-4 2
		2.0429	3	1 5 1
		2.0253	7	-2-1 4
		2.0169	3	4 2 4
16	2.0097	2.0086	8	2 0 5
		2.0040	4	3 5 2
		1.9985	5	-3-2 3
		1.9879	2	-1 4 2
8	1.9338	1.9346	4	5 2 1
		1.9311	3	3-1 4
		1.9095	2	-2-5 1
		1.9086	2	5 3 2
6	1.8966	1.9051	4	0 5 1
		1.8908	2	-1 1 5
		1.8889	2	1 5 3
7	1.8706	1.8745	6	5 2 0
		1.8480	3	-4-3 2
		1.8435	2	-1 4 3
7	1.8378	1.8385	3	5 1 0
		1.8350	2	0-4 3
		1.8259	2	4-1 3
		1.8122	2	3-3 1
		1.8057	2	2 5 4
		1.8012	2	1-3 4
9	1.7989	1.7995	3	5 1 3
		1.7962	2	0-2 5
		1.7926	2	4 5 0
		1.7734	2	-3-1 4
		1.7705	3	1 4 5
10	1.7656	1.7692	2	1-2 5
		1.7647	2	-5-2 1
		1.7598	2	-3 0 4
		1.7549	5	4 1 5
		1.7429	8	1 5 4
11	1.7411	1.7417	3	-5-1 1
		1.7359	2	-4-1 3
		1.7209	4	-4-2 3
8	1.7141	1.7166	3	3-2 4
		1.7134	4	-4-4 2
		1.6960	2	2 6 0
		1.6899	2	-3 1 4
7	1.6817	1.6852	2	4-1 4
		1.6772	2	0 2 6
		1.6689	2	2 6 3
		1.6671	4	3 6 0
5	1.6550	1.6623	2	1 6 0
		1.6429	2	0-1 6
		1.6417	2	3-3 3
		1.6116	2	5 5 0
		1.6068	2	-4 1 3
8	1.6073	1.6032	2	-4 2 2
		1.5997	2	3 4 6
		1.5974	2	-1-6 1
		1.5907	3	0 3 6
		1.5898	9	5 0 4
12	1.5870	1.5867	2	1 5 5
		1.5844	2	4 6 0
		1.5800	2	-1-1 6
		1.5700	2	5 4 5
		1.5586	2	6 2 0
9	1.5565	1.5573	3	3-4 1
		1.5564	3	6 1 1
		1.5457	3	-4-1 4
8	1.5419	1.5441	5	-3-1 5
		1.5427	2	0-2 6
		1.5324	2	5 6 2
5	1.5110	1.5155	2	-2-6 2
		1.5052	2	-1-2 6
8	1.4888	1.4940	3	5 5 5
		1.4900	4	4 0 6
		1.4778	2	-4-3 4
		1.4769	3	3 3 7
8	1.4698	1.4693	2	5 6 0
		1.4685	2	-5 2 0
		1.4608	4	3 7 3
		1.4593	5	2-5 2
8	1.4543	1.4588	4	4 5 6
		1.4559	2	-3 3 4
		1.4370	2	1 5 6
7	1.4207	1.4234	3	6 2 5

*Calculated lines with $I < 2$ are omitted.

Table 3a. Sample and crystal data for carlsonite.*

Diffractometer	Rigaku R-Axis Rapid II	
X-ray radiation/power	Mo$K\alpha$ (λ = 0.71075 Å)/50 kV, 40 mA	
Temperature	298(2) K	
Structural formula	$(NH_4)_5Fe^{3+}{}_3O(SO_4)_6 \cdot 7H_2O$	
Space group	*P*-1	
Unit-cell dimensions	*a* = 9.5927(2) Å	α = 93.250(7)°
	b = 9.7679(3) Å	β = 95.258(7)°
	c = 18.3995(13) Å	γ = 117.993(8)°
V	1506.15(16) Å^3	
Z	2	
Density (for above formula)	2.153 g cm^{-3}	
Absorption coefficient	1.968 mm^{-1}	
F(000)	998	
Crystal size	200 x 130 x 110 µm	
θ range	3.07 to 27.45°	
Index ranges	$-12 \le h \le 12$, $-12 \le k \le 12$, $-23 \le l \le 23$	
Reflections collected / unique	28480 / 6869; R_{int} = 0.017	
Reflections with $F_o > 4\sigma(F)$	6430	
Completeness to θ = 27.45°	99.7%	
Max. and min. transmission	0.813 and 0.694	
Refinement method	Full-matrix least-squares on F^2	
Parameters refined/restrained	71/517	
GoF	1.124	
Final *R* indices [$F_o > 4\sigma(F)$]	R_1 = 0.0297, wR_2 = 0.0812	
R indices (all data)	R_1 = 0.0314, wR_2 = 0.0826	
Largest diff. peak / hole	+0.94 / –0.77 *e*/A^3	

*$R_{int} = \Sigma|F_o^2 - F_o^2(\text{mean})|/\Sigma[F_o^2]$. GoF = $S = \{\Sigma[w(F_o^2 - F_c^2)^2]/(n-p)\}^{1/2}$. $R_1 = \Sigma||F_o| - |F_c||/\Sigma|F_o|$. $wR_2 = \{\Sigma[w(F_o^2 - F_c^2)^2]/\Sigma[w(F_o^2)^2]\}^{1/2}$; $w = 1/[\sigma^2(F_o^2) + (aP)^2 + bP]$ where *a* is 0.0505, *b* is 1.0203 and *P* is $[2F_c^2 + \text{Max}(F_o^2, 0)]/3$

Table 3b. Sample and crystal data for huizingite-(Al).*

Diffractometer	Rigaku R-Axis Rapid II	
X-ray radiation/power	Mo$K\alpha$ (λ = 0.71075 Å)/50 kV, 40 mA	
Temperature	298(2) K	
Structural formula	$[(NH_4)_9(SO_4)_2][(Al_{1.72}Fe_{1.28})_3(SO_4)_6(OH)_2(H_2O)_4]$	
Space group	*P*-1	
Unit-cell dimensions	*a* = 9.7093(3) Å	α = 77.231(5)°
	b = 10.4341(3) Å	β = 74.860(5)°
	c = 10.7027(8) Å	γ = 66.104(5)°
V	948.73(9) Å^3	
Z	1	
Density (for above formula)	2.021 g cm^{-3}	
Absorption coefficient	1.113 mm^{-1}	
F(000)	597	
Crystal size	90 x 60 x 30 µm	
θ range	3.12 to 27.45°	
Index ranges	$-12 \le h \le 12$, $-13 \le k \le 13$, $-13 \le l \le 13$	
Reflections collected / unique	18529 / 4323; R_{int} = 0.046	
Reflections with $F_o > 4\sigma(F)$	3543	
Completeness to θ = 27.45°	99.6%	
Max. and min. transmission	0.967 and 0.906	
Refinement method	Full-matrix least-squares on F^2	
Parameters refined/restrained	342 / 50	
GoF	1.059	
Final *R* indices [$F_o > 4\sigma(F)$]	R_1 = 0.0399, wR_2 = 0.0874	
R indices (all data)	R_1 = 0.0519, wR_2 = 0.0925	
Largest diff. peak / hole	+0.40 / –0.50 *e*/A^3	

*$R_{int} = \Sigma|F_o^2\text{-}F_o^2(\text{mean})|/\Sigma[F_o^2]$. GoF = $S = \{\Sigma[w(F_o^2 - F_c^2)^2]/(n-p)\}^{1/2}$. $R_1 = \Sigma||F_o|\text{-}|F_c||/\Sigma|F_o|$. $wR_2 = \{\Sigma[w(F_o^2 - F_c^2)^2]/\Sigma[w(F_o^2)^2]\}^{1/2}$; $w = 1/[\sigma^2(F_o^2) + (aP)^2 + bP]$ where *a* is 0.0375, *b* is 1.0704 and *P* is $[2F_c^2 + \text{Max}(F_o^2,0)]/3$

Table 4a. Atom coordinates and displacement parameters (Å^2) for carlsonite.

	x/*a*	*y*/*b*	*z*/*c*	U_{eq}	U^{11}	U^{22}	U^{33}	U^{23}	U^{13}	U^{12}
Fe1	0.62121(3)	0.25279(3)	0.24651(2)	0.01520(7)	0.01411(13)	0.01468(14)	0.01811(14)	0.00311(10)	0.00349(10)	0.00755(11)
Fe2	0.36807(3)	0.39286(3)	0.26517(2)	0.01689(7)	0.01465(14)	0.01465(14)	0.02217(14)	0.00177(10)	0.00219(10)	0.00774(11)
Fe3	0.24002(3)	0.00884(3)	0.25780(2)	0.01645(7)	0.01478(14)	0.01498(14)	0.02002(14)	0.00208(10)	0.00407(10)	0.00715(11)
S1	0.42868(6)	-0.06325(6)	0.13719(3)	0.01942(11)	0.0201(2)	0.0189(2)	0.0188(2)	-0.00139(17)	0.00331(17)	0.00918(19)
S2	0.71360(6)	0.54664(6)	0.36759(3)	0.01832(10)	0.0169(2)	0.0167(2)	0.0190(2)	0.00004(17)	0.00171(17)	0.00638(18)
S3	0.51278(6)	-0.00006(6)	0.36580(3)	0.01964(11)	0.0211(2)	0.0206(2)	0.0191(2)	0.00663(18)	0.00275(18)	0.01097(19)
S4	0.06836(6)	0.13994(6)	0.14676(3)	0.01828(10)	0.0176(2)	0.0207(2)	0.0179(2)	0.00111(17)	0.00119(17)	0.01052(19)
S5	0.59911(6)	0.49178(6)	0.13715(3)	0.02132(11)	0.0215(2)	0.0221(2)	0.0214(2)	0.00860(19)	0.00461(18)	0.0104(2)
S6	0.12297(6)	0.18539(6)	0.37145(3)	0.01986(11)	0.0205(2)	0.0248(2)	0.0188(2)	0.00278(18)	0.00495(17)	0.0140(2)
O1	0.4974(2)	-0.1674(2)	0.13588(11)	0.0371(4)	0.0406(10)	0.0300(9)	0.0522(11)	0.0044(8)	0.0200(8)	0.0239(8)
O2	0.3344(2)	-0.0787(3)	0.06780(10)	0.0440(5)	0.0403(10)	0.0527(12)	0.0252(8)	0.0022(8)	-0.0062(7)	0.0130(9)
O3	0.55703(19)	0.10241(18)	0.15437(8)	0.0263(3)	0.0268(8)	0.0218(8)	0.0243(7)	-0.0015(6)	0.0095(6)	0.0058(6)
O4	0.32513(18)	-0.10129(17)	0.19731(8)	0.0226(3)	0.0218(7)	0.0192(7)	0.0282(7)	0.0017(6)	0.0093(6)	0.0099(6)
O5	0.7032(3)	0.5393(2)	0.44527(10)	0.0418(4)	0.0596(12)	0.0411(10)	0.0236(8)	0.0061(7)	0.0136(8)	0.0216(10)
O6	0.8492(2)	0.6918(2)	0.35524(10)	0.0317(4)	0.0224(8)	0.0250(8)	0.0379(9)	0.0040(7)	0.0068(7)	0.0027(7)
O7	0.7256(2)	0.40985(19)	0.33607(9)	0.0298(4)	0.0290(8)	0.0281(8)	0.0333(8)	-0.0112(7)	-0.0089(6)	0.0182(7)
O8	0.5675(2)	0.54338(19)	0.32936(11)	0.0351(4)	0.0231(8)	0.0224(8)	0.0565(11)	-0.0096(8)	-0.0120(7)	0.0126(7)
O9	0.5916(2)	0.0827(2)	0.43761(9)	0.0355(4)	0.0345(9)	0.0451(10)	0.0225(8)	-0.0019(7)	-0.0020(7)	0.0171(8)
O10	0.4965(2)	-0.15715(19)	0.35909(9)	0.0313(4)	0.0373(9)	0.0232(8)	0.0369(9)	0.0121(7)	0.0061(7)	0.0162(7)
O11	0.60687(18)	0.08306(18)	0.30713(8)	0.0225(3)	0.0214(7)	0.0243(7)	0.0266(7)	0.0106(6)	0.0075(6)	0.0133(6)
O12	0.35299(19)	-0.0077(2)	0.35345(8)	0.0267(3)	0.0226(7)	0.0374(9)	0.0251(7)	0.0133(7)	0.0079(6)	0.0166(7)
O13	0.0973(3)	0.1789(2)	0.07287(9)	0.0405(4)	0.0583(12)	0.0505(11)	0.0245(8)	0.0128(8)	0.0146(8)	0.0332(10)
O14	-0.10093(18)	0.0754(2)	0.15429(10)	0.0295(3)	0.0172(7)	0.0282(8)	0.0389(9)	-0.0047(7)	0.0006(6)	0.0089(6)
O15	0.1212(2)	0.02310(19)	0.16453(9)	0.0269(3)	0.0307(8)	0.0247(8)	0.0281(8)	-0.0049(6)	-0.0063(6)	0.0181(7)
O16	0.15765(18)	0.28191(17)	0.20106(9)	0.0244(3)	0.0203(7)	0.0192(7)	0.0325(8)	-0.0032(6)	-0.0042(6)	0.0105(6)
O17	0.5322(3)	0.4022(3)	0.06609(11)	0.0589(6)	0.0678(15)	0.0686(16)	0.0312(10)	-0.0096(10)	-0.0107(10)	0.0299(13)
O18	0.7109(2)	0.6528(2)	0.13069(12)	0.0401(4)	0.0342(9)	0.0261(9)	0.0648(12)	0.0245(9)	0.0180(9)	0.0143(8)
O19	0.4691(2)	0.4878(2)	0.17653(11)	0.0390(4)	0.0364(10)	0.0509(11)	0.0501(11)	0.0331(9)	0.0238(8)	0.0316(9)
O20	0.68350(19)	0.42422(19)	0.18223(9)	0.0274(3)	0.0233(7)	0.0277(8)	0.0376(9)	0.0173(7)	0.0103(6)	0.0148(7)
O21	0.1458(2)	0.1434(2)	0.44455(9)	0.0317(4)	0.0362(9)	0.0367(9)	0.0227(8)	0.0091(7)	0.0041(7)	0.0172(8)
O22	-0.0144(2)	0.2120(2)	0.36220(9)	0.0349(4)	0.0331(9)	0.0534(11)	0.0330(9)	0.0053(8)	0.0072(7)	0.0323(9)
O23	0.2705(2)	0.32705(19)	0.35946(8)	0.0279(3)	0.0315(8)	0.0230(8)	0.0241(7)	-0.0007(6)	0.0077(6)	0.0086(7)
O24	0.09649(18)	0.05547(18)	0.31503(8)	0.0248(3)	0.0195(7)	0.0240(8)	0.0291(8)	-0.0028(6)	0.0065(6)	0.0089(6)

720	O25	0.41093(16)	0.21995(16)	0.25570(7)	0.0161(3)	0.0141(6)	0.0146(6)	0.0205(6)	0.0024(5)	0.0033(5)	0.0075(5)
721	OW1	0.85062(18)	0.28090(18)	0.23993(9)	0.0228(3)	0.0183(7)	0.0251(8)	0.0286(8)	0.0043(6)	0.0048(6)	0.0129(6)
722	HW1a	0.904(3)	0.290(3)	0.2794(12)	0.027						
723	HW1b	0.857(3)	0.219(3)	0.2110(13)	0.027						
724	OW2	0.3064(2)	0.5696(2)	0.27352(10)	0.0319(4)	0.0327(9)	0.0234(8)	0.0420(9)	-0.0049(7)	-0.0087(7)	0.0186(7)
725	HW2a	0.249(3)	0.578(4)	0.2395(14)	0.038						
726	HW2b	0.353(3)	0.655(3)	0.2965(15)	0.038						
727	OW3	0.0645(2)	-0.2161(2)	0.26112(11)	0.0363(4)	0.0333(9)	0.0187(8)	0.0495(11)	0.0008(7)	0.0231(8)	0.0036(7)
728	HW3a	0.054(4)	-0.296(3)	0.2366(16)	0.044						
729	HW3b	0.003(4)	-0.254(4)	0.2902(15)	0.044						
730	OW4	0.0689(2)	0.5530(2)	0.17521(13)	0.0443(5)	0.0374(11)	0.0252(9)	0.0635(13)	0.0037(9)	-0.0073(9)	0.0120(8)
731	HW4a	0.042(4)	0.587(4)	0.1395(16)	0.053						
732	HW4b	0.003(4)	0.468(3)	0.1749(19)	0.053						
733	OW5	0.8216(5)	0.3194(4)	0.05751(17)	0.0793(9)	0.106(3)	0.0638(18)	0.0733(19)	-0.0013(14)	0.0157(17)	0.0453(18)
734	HW5a	0.894(5)	0.323(6)	0.024(2)	0.095						
735	HW5b	0.746(4)	0.237(5)	0.025(2)	0.095						
736	OW6	0.1324(8)	0.5631(6)	0.4345(4)	0.171(3)	0.215(6)	0.120(4)	0.202(5)	-0.087(4)	-0.095(5)	0.132(4)
737	HW6a	0.037(9)	0.507(10)	0.454(4)	0.205						
738	HW6b	0.100(9)	0.548(10)	0.3879(19)	0.205						
739	OW7	0.0086(3)	0.2942(3)	-0.07344(12)	0.0488(5)	0.0386(11)	0.0510(13)	0.0443(11)	0.0053(10)	0.0016(9)	0.0120(10)
740	HW7a	0.079(3)	0.283(4)	-0.089(2)	0.059						
741	HW7b	-0.069(3)	0.211(3)	-0.076(2)	0.059						
742	N1	0.4767(3)	0.2788(3)	0.50578(12)	0.0367(5)	0.0395(12)	0.0447(13)	0.0306(11)	0.0137(9)	0.0080(9)	0.0223(11)
743	HN1a	0.380(2)	0.263(4)	0.4955(16)	0.044						
744	HN1b	0.538(3)	0.370(3)	0.4912(16)	0.044						
745	HN1c	0.497(4)	0.279(3)	0.5524(11)	0.044						
746	HN1d	0.497(4)	0.211(3)	0.4809(15)	0.044						
747	N2	0.2935(3)	0.1274(3)	-0.02010(11)	0.0337(4)	0.0356(11)	0.0352(12)	0.0266(10)	-0.0011(9)	0.0064(9)	0.0139(10)
748	HN2a	0.314(3)	0.065(3)	0.0086(14)	0.040						
749	HN2b	0.223(3)	0.142(3)	0.0058(15)	0.040						
750	HN2c	0.375(3)	0.211(3)	-0.0159(16)	0.040						
751	HN2d	0.242(3)	0.072(3)	-0.0594(12)	0.040						
752	N3	0.2574(3)	0.5122(3)	0.05027(14)	0.0462(6)	0.0539(16)	0.0478(15)	0.0372(12)	0.0040(11)	-0.0012(11)	0.0259(13)
753	HN3a	0.210(4)	0.559(4)	0.0251(16)	0.055						
754	HN3b	0.326(3)	0.508(4)	0.0219(16)	0.055						

HN3c	0.317(3)	0.587(3)	0.0872(14)	0.055						
HN3d	0.188(3)	0.432(3)	0.0637(18)	0.055						
N4	0.1104(3)	-0.1644(3)	0.47709(12)	0.0364(5)	0.0345(12)	0.0410(13)	0.0329(11)	0.0024(9)	0.0005(9)	0.0183(10)
HN4a	0.197(3)	-0.131(3)	0.5133(13)	0.044						
HN4b	0.101(4)	-0.249(3)	0.4560(15)	0.044						
HN4c	0.131(4)	-0.092(3)	0.4508(14)	0.044						
HN4d	0.029(3)	-0.185(3)	0.5018(15)	0.044						
N5	0.7340(2)	-0.1376(2)	0.25778(11)	0.0249(4)	0.0269(10)	0.0240(9)	0.0268(9)	0.0098(8)	0.0084(8)	0.0130(8)
HN5a	0.818(2)	-0.075(3)	0.2489(14)	0.030						
HN5b	0.733(3)	-0.199(3)	0.2887(13)	0.030						
HN5c	0.665(3)	-0.186(3)	0.2213(11)	0.030						
HN5d	0.692(3)	-0.088(3)	0.2820(13)	0.030						

Table 4b. Atom coordinates and displacement parameters ($Å^2$) for huizingite-(Al).

	x/*a*	*y*/*b*	*z*/*c*	U_{eq}	U^{11}	U^{22}	U^{33}	U^{23}	U^{13}	U^{12}
Al1	0.5	0.5	0.0	0.0184(3)	0.0193(4)	0.0182(4)	0.0178(4)	-0.0042(3)	-0.0023(3)	-0.0069(3)
Al2	0.40551(6)	0.74296(5)	0.21230(5)	0.01774(18)	0.0188(3)	0.0186(3)	0.0167(3)	-0.0022(2)	-0.0046(2)	-0.0070(2)
S1	0.37237(7)	0.24458(7)	0.06816(6)	0.02067(16)	0.0203(3)	0.0226(3)	0.0197(3)	-0.0017(3)	-0.0034(3)	-0.0094(3)
S2	0.19631(8)	0.76866(7)	0.01591(7)	0.02286(16)	0.0212(3)	0.0237(3)	0.0241(3)	-0.0041(3)	-0.0083(3)	-0.0059(3)
S3	0.69632(8)	0.54010(7)	0.34623(7)	0.02388(16)	0.0233(3)	0.0260(4)	0.0229(3)	-0.0004(3)	-0.0087(3)	-0.0084(3)
S4	0.82969(8)	0.87469(8)	0.46665(7)	0.02857(18)	0.0290(4)	0.0314(4)	0.0258(4)	-0.0049(3)	-0.0064(3)	-0.0104(3)
O1	0.2184(2)	0.2426(2)	0.0949(2)	0.0316(5)	0.0237(10)	0.0381(12)	0.0351(12)	-0.0009(10)	-0.0041(9)	-0.0163(9)
O2	0.4652(2)	0.1410(2)	0.15867(19)	0.0298(5)	0.0316(11)	0.0315(11)	0.0268(10)	0.0050(9)	-0.0129(9)	-0.0121(9)
O3	0.3605(2)	0.3897(2)	0.07501(19)	0.0273(4)	0.0303(11)	0.0242(10)	0.0275(10)	-0.0066(9)	0.0025(8)	-0.0135(8)
O4	0.5546(2)	0.7897(2)	0.06772(18)	0.0270(4)	0.0332(11)	0.0302(11)	0.0219(10)	-0.0067(9)	-0.0005(8)	-0.0174(9)
O5	0.1315(3)	0.8847(2)	-0.0795(2)	0.0426(6)	0.0561(15)	0.0300(12)	0.0404(13)	-0.0019(10)	-0.0321(12)	-0.0020(11)
O6	0.0895(2)	0.7015(3)	0.0888(2)	0.0421(6)	0.0299(12)	0.0458(14)	0.0546(15)	-0.0169(12)	0.0065(11)	-0.0218(10)
O7	0.3338(2)	0.6619(2)	-0.05358(19)	0.0277(4)	0.0259(10)	0.0286(11)	0.0261(10)	-0.0075(9)	-0.0053(8)	-0.0055(8)
O8	0.2471(2)	0.8229(2)	0.1065(2)	0.0300(5)	0.0313(11)	0.0289(11)	0.0316(11)	-0.0073(9)	-0.0158(9)	-0.0052(9)
O9	0.8258(3)	0.5652(3)	0.2550(3)	0.0496(6)	0.0284(12)	0.0644(17)	0.0488(15)	0.0017(13)	-0.0001(11)	-0.0190(12)
O10	0.7139(3)	0.5238(2)	0.4811(2)	0.0409(6)	0.0540(15)	0.0393(13)	0.0305(12)	-0.0002(10)	-0.0237(11)	-0.0112(11)
O11	0.6796(3)	0.4144(2)	0.3211(2)	0.0402(6)	0.0463(14)	0.0262(11)	0.0528(15)	-0.0047(11)	-0.0229(11)	-0.0101(10)

788	O12	0.5535(2)	0.6654(2)	0.3284(2)	0.0289(5)	0.0285(11)	0.0280(11)	0.0294(11)	-0.0049(9)	-0.0129(9)	-0.0046(8)
789	O13	0.8548(4)	0.7691(3)	0.5804(3)	0.0744(10)	0.130(3)	0.0511(17)	0.0597(18)	0.0213(15)	-0.0568(19)	-0.0426(19)
790	O14	0.6914(3)	0.8920(3)	0.4237(2)	0.0486(6)	0.0343(13)	0.0790(19)	0.0398(13)	-0.0089(13)	-0.0069(11)	-0.0279(13)
791	O15	0.9596(3)	0.8390(4)	0.3573(3)	0.0640(9)	0.0256(13)	0.110(3)	0.0517(16)	-0.0445(17)	-0.0001(12)	-0.0073(14)
792	O16	0.8101(3)	0.0103(3)	0.5023(2)	0.0485(6)	0.0687(17)	0.0422(14)	0.0407(14)	-0.0108(12)	0.0045(12)	-0.0332(13)
793	OH1	0.4586(2)	0.5597(2)	0.16627(19)	0.0228(4)	0.0241(10)	0.0224(10)	0.0230(10)	-0.0026(8)	-0.0092(8)	-0.0069(8)
794	H1	0.523(3)	0.503(3)	0.203(3)	0.027						
795	OW1	0.3499(3)	0.9294(2)	0.2612(2)	0.0303(5)	0.0384(12)	0.0282(11)	0.0246(11)	-0.0031(9)	0.0000(9)	-0.0164(9)
796	HW1a	0.295(3)	0.946(4)	0.333(3)	0.036						
797	HW1b	0.386(4)	0.988(3)	0.235(3)	0.036						
798	OW2	0.2507(2)	0.7242(2)	0.3647(2)	0.0322(5)	0.0260(11)	0.0301(12)	0.0363(12)	0.0034(10)	-0.0061(10)	-0.0098(9)
799	HW2a	0.276(4)	0.664(3)	0.422(3)	0.039						
800	HW2b	0.159(3)	0.756(3)	0.366(3)	0.039						
801	N1	0.4800(3)	0.7877(3)	0.6057(3)	0.0382(6)	0.0377(16)	0.0347(15)	0.0448(17)	-0.0049(14)	-0.0088(13)	-0.0155(13)
802	HN1a	0.555(3)	0.798(3)	0.547(3)	0.046						
803	HN1b	0.486(4)	0.794(3)	0.686(2)	0.046						
804	HN1c	0.393(3)	0.859(3)	0.586(3)	0.046						
805	HN1d	0.465(4)	0.709(3)	0.609(3)	0.046						
806	N2	0.0275(4)	0.8436(4)	0.7176(3)	0.0474(8)	0.054(2)	0.063(2)	0.0396(17)	0.0096(16)	-0.0211(15)	-0.0368(17)
807	HN2a	0.107(3)	0.765(3)	0.716(4)	0.057						
808	HN2b	0.008(4)	0.890(3)	0.783(3)	0.057						
809	HN2c	-0.056(3)	0.835(4)	0.712(3)	0.057						
810	HN2d	0.054(4)	0.903(3)	0.646(3)	0.057						
811	N3	0.1115(4)	0.5045(4)	0.3225(3)	0.0516(8)	0.063(2)	0.052(2)	0.055(2)	0.0019(17)	-0.0280(18)	-0.0311(18)
812	HN3a	0.142(4)	0.517(4)	0.389(3)	0.062						
813	HN3b	0.127(4)	0.409(2)	0.338(4)	0.062						
814	HN3c	0.019(3)	0.552(3)	0.318(4)	0.062						
815	HN3d	0.178(4)	0.515(4)	0.251(3)	0.062						
816	N4	0.2297(3)	0.1194(3)	0.8502(3)	0.0363(6)	0.0359(15)	0.0386(16)	0.0396(16)	-0.0118(13)	-0.0132(13)	-0.0121(13)
817	HN4a	0.261(4)	0.126(3)	0.765(2)	0.044						
818	HN4b	0.230(4)	0.039(2)	0.888(3)	0.044						
819	HN4c	0.134(2)	0.182(3)	0.865(3)	0.044						

HN4d	0.286(3)	0.150(3)	0.881(3)	0.044						
N5	0.0000	0.5000	0.0000	0.0552(13)	0.072(4)	0.037(3)	0.050(3)	-0.014(2)	-0.030(3)	0.002(3)
HN5a	0.044(10)	0.555(9)	0.013(10)	0.066						
HN5b	0.061(7)	0.419(5)	0.039(6)	0.066						
HN5c	0.059(8)	0.494(9)	-0.081(4)	0.066						

Site occupancies: Al1: Al/Fe 0.597/0.403(5), Al2: Al/Fe 0.562/0.438(4), HN5A: 0.50(9), HN5B: 0.69(8), HN5C: 0.58(9)

Table 5a. Selected bond distances (Å) for carlsonite.

$NH_4$1–O5	2.830(3)	S1–O1	1.4492(17)	Fe1–O25	1.9136(13)
$NH_4$1–O10	2.858(3)	S1–O2	1.4522(18)	Fe1–O20	1.9937(15)
$NH_4$1–O21	2.886(3)	S1–O3	1.4949(16)	Fe1–O11	2.0087(14)
$NH_4$1–O9	2.902(3)	S1–O4	1.5000(15)	Fe1–O7	2.0100(16)
$NH_4$1–O5	3.151(3)	<S1–O>	1.4741	Fe1–O3	2.0220(15)
$NH_4$1–OW6	3.355(6)			Fe1–OW1	2.1019(15)
$NH_4$1–O23	3.380(3)	S2–O5	1.4452(17)	<Fe1–O>	2.0083
<$NH_4$1–O>	3.052	S2–O6	1.4537(17)		
		S2–O7	1.4844(16)	Fe2–O25	1.9192(13)
$NH_4$2–O2	2.796(3)	S2–O8	1.4952(16)	Fe2–O8	1.9911(17)
$NH_4$2–O17	2.836(3)	<S2–O>	1.4696	Fe2–O16	2.0014(15)
$NH_4$2–O13	2.847(3)			Fe2–O19	2.0191(17)
$NH_4$2–O14	2.934(3)	S3–O9	1.4467(17)	Fe2–O23	2.0390(16)
$NH_4$2–O1	2.976(3)	S3–O10	1.4643(17)	Fe2–OW2	2.0735(16)
$NH_4$2–O18	3.052(3)	S3–O11	1.4930(15)	<Fe2–O>	2.0072
<$NH_4$2–O>	2.907	S3–O12	1.4944(16)		
		<S3–O>	1.4746	Fe3–O25	1.9465(14)
$NH_4$3–OW5	2.911(4)			Fe3–O4	1.9793(14)
$NH_4$3–O13	2.951(3)	S4–O13	1.4489(17)	Fe3–O24	2.0030(15)
$NH_4$3–O17	2.961(4)	S4–O14	1.4642(16)	Fe3–O15	2.0200(15)
$NH_4$3–OW7	3.016(3)	S4–O15	1.4907(15)	Fe3–O12	2.0360(15)
$NH_4$3–O19	3.038(3)	S4–O16	1.4920(15)	Fe3–OW3	2.0560(17)
$NH_4$3–O1	3.096(3)	<S4–O>	1.4740	<Fe2–O>	2.0068
$NH_4$3–OW4	3.170(4)				
$NH_4$3–O17	3.278(4)	S5–O17	1.4410(21)	Hydrogen bonds	
<$NH_4$3–O>	3.053	S5–O18	1.4491(18)	OW1···O22	2.765(2)
		S5–O19	1.4846(17)	OW1···O14	2.717(2)
$NH_4$4–OW6	2.838(5)	S5–O20	1.4897(16)	OW2···OW4	2.711(3)
$NH_4$4–O9	2.858(3)	<S5–O>	1.4661	OW2···O10	2.713(3)
$NH_4$4–O6	2.930(3)			OW3···OW4	2.699(3)
$NH_4$4–O21	2.966(3)	S6–O21	1.4555(16)	OW3···O6	2.676(2)
$NH_4$4–O21	3.042(3)	S6–O22	1.4557(16)	OW4···OW7	2.719(3)
$NH_4$4–O22	3.172(3)	S6–O23	1.4902(17)	OW4···OW1	2.908(3)
$NH_4$4–O12	3.310(3)	S6–O24	1.5007(15)	OW5···OW7	3.198(4)
<$NH_4$4–O>	3.017	<S6–O>	1.4755	OW5···O2	2.921(4)
				OW6···none	
$NH_4$5–O14	2.894(3)			OW6···none	
$NH_4$5–O1	2.939(3)			OW7···O18	2.808(3)
$NH_4$5–O18	2.940(3)			OW7···O2	2.976(3)
$NH_4$5–O6	2.986(3)				
$NH_4$5–O10	3.018(3)				
$NH_4$5–O11	3.067(2)				
$NH_4$5–O24	3.116(3)				
$NH_4$5–O8	3.189(3)				
<$NH_4$5–O>	3.019				

Table 5b. Selected bond distances (Å) for huizingite-(Al).

$NH_4$1–O14	2.824(4)	$NH_4$4–O14	2.847(4)	S1–O1	1.455(2)
$NH_4$1–O11	2.957(4)	$NH_4$4–O5	2.860(4)	S1–O2	1.457(2)
$NH_4$1–O2	3.008(4)	$NH_4$4–O6	2.883(4)	S1–O3	1.488(2)
$NH_4$1–O14	3.056(4)	$NH_4$4–O4	2.999(3)	S1–O4	1.4938(19)
$NH_4$1–O10	3.081(4)	$NH_4$4–O15	3.092(4)	<Si1–O>	1.473
$NH_4$1–O16	3.086(4)	$NH_4$4–O2	3.100(3)		
$NH_4$1–O12	3.281(4)	$NH_4$4–O9	3.103(4)	S2–O5	1.441(2)
<$NH_4$1–O>	3.042	$NH_4$4–O1	3.122(3)	S2–O6	1.449(2)
		<$NH_4$4–O>	3.001	S2–O7	1.490(2)
$NH_4$2–O5	2.797(4)			S2–O8	1.491(2)
$NH_4$2–O13	2.902(4)	$NH_4$5–O1(×2)	2.837(2)	<Si2–O>	1.468
$NH_4$2–O16	2.962(4)	$NH_4$5–O9(×2)	2.872(3)		
$NH_4$2–O1	2.996(4)	$NH_4$5–O6(×2)	2.979(2)	S3–O9	1.454(2)
$NH_4$2–O11	3.030(4)	<$NH_4$5–O>	2.896	S3–O10	1.462(2)
$NH_4$2–O16	3.254(4)			S3–O11	1.473(2)
$NH_4$2–O15	3.277(5)	Al1–OH1(×2)	1.9051(19)	S3–O12	1.493(2)
<$NH_4$2–O>	3.031	Al1–O7(×2)	1.906(2)	<Si3–O>	1.471
		Al1–O3(×2)	2.0225(19)		
$NH_4$3–O13	2.729(4)	<Al1–O>	1.945	S4–O13	1.449(3)
$NH_4$3–O9	2.836(4)			S4–O14	1.462(2)
$NH_4$3–O6	2.860(4)	Al2–OH1	1.9107(19)	S4–O15	1.463(3)
$NH_4$3–O10	2.926(4)	Al2–OW2	1.943(2)	S4–O16	1.472(2)
$NH_4$3–O3	3.163(4)	Al2–O4	1.9480(19)	<Si4–O>	1.462
$NH_4$3–OW2	3.251(4)	Al2–O8	1.948(2)		
$NH_4$3–O15	3.258(5)	Al2–OW1	1.950(2)	Hydrogen bonds	
<$NH_4$3–O>	3.003	Al2–O12	1.952(2)	OH1···O11	2.786(3)
		<Al2–O>	1.942	OW1···O16	2.660(3)
				OW1···O2	2.761(3)
				OW2···O10	2.688(3)
				OW2···O15	2.601(3)

Table 6a. Bond distances and angles for N–H–O bonds in carlsonite.

N–H···O	*d*(N–H)	*d*(H···O)	*d*(N–O)	<N–H···O	NH_4···O bonding*
N1-HN1a···O21	0.87(2)	2.08(2)	2.886(3)	155(3)	hydrogen bond
N1-HN1a···O5	0.87(2)	2.63(3)	3.151(3)	120(2)	electrostatic bond
N1-HN1a···O23	0.87(2)	2.84(3)	3.380(3)	122(2)	electrostatic bond
N1-HN1b···O5	0.88(2)	1.97(2)	2.830(3)	163(3)	hydrogen bond
N1-HN1b···OW6	0.88(2)	3.07(3)	3.357(6)	101(2)	electrostatic bond
N1-HN1c···O10	0.86(2)	2.09(2)	2.858(3)	149(3)	hydrogen bond
N1-HN1d···O9	0.89(2)	2.02(2)	2.902(3)	168(3)	hydrogen bond
N2-HN2a···O2	0.91(2)	1.89(2)	2.796(3)	174(3)	hydrogen bond
N2-HN2b···O13	0.92(2)	1.93(2)	2.847(3)	172(3)	hydrogen bond
N2-HN2c···O17	0.82(2)	2.16(2)	2.836(3)	140(3)	hydrogen bond
N2-HN2c···O1	0.82(2)	2.72(3)	2.976(3)	100(2)	electrostatic bond
N2-HN2c···O18	0.82(2)	2.82(3)	3.052(3)	99(2)	electrostatic bond
N2-HN2d···O14	0.84(2)	2.10(2)	2.934(3)	176(3)	hydrogen bond
N3-HN3a···OW5	0.90(2)	2.07(2)	2.911(4)	156(3)	hydrogen bond
N3-HN3b···O17	0.89(2)	2.16(3)	2.961(4)	148(3)	hydrogen bond
N3-HN3b···O17	0.89(2)	2.71(3)	3.278(4)	123(3)	electrostatic bond
N3-HN3c···O1	0.90(2)	2.26(2)	3.096(3)	154(3)	hydrogen bond
N3-HN3c···O19	0.90(2)	2.61(3)	3.038(3)	110(2)	electrostatic bond
N3-HN3d···O13	0.82(2)	2.23(2)	2.951(3)	147(3)	hydrogen bond
N3-HN3d···OW7	0.82(2)	2.79(3)	3.016(3)	98(2)	electrostatic bond
N3-HN3d···OW4	0.82(2)	2.88(3)	3.170(4)	103(2)	electrostatic bond
N4-HN4a···O9	0.93(2)	1.97(2)	2.858(3)	160(3)	hydrogen bond
N4-HN4b···OW6	0.86(2)	2.01(2)	2.839(5)	161(3)	hydrogen bond
N4-HN4b···O6	0.86(2)	2.71(3)	2.930(3)	96(2)	electrostatic bond
N4-HN4c···O21	0.84(2)	2.24(2)	2.966(3)	144(3)	hydrogen bond
N4-HN4c···O12	0.84(2)	2.76(3)	3.310(3)	124(2)	electrostatic bond
N4-HN4d···O21	0.89(2)	2.20(2)	3.042(3)	158(3)	hydrogen bond
N4-HN4d···O22	0.89(2)	2.54(3)	3.172(3)	129(2)	electrostatic bond
N5-HN5a···O14	0.79(2)	2.30(2)	2.894(3)	133(2)	electrostatic bond
N5-HN5a···O24	0.79(2)	2.51(2)	3.116(3)	135(2)	electrostatic bond
N5-HN5b···O6	0.85(2)	2.21(2)	2.986(3)	152(2)	hydrogen bond
N5-HN5b···O8	0.85(2)	2.47(2)	3.189(3)	143(2)	electrostatic bond
N5-HN5c···O1	0.84(2)	2.22(2)	2.939(3)	144(2)	hydrogen bond
N5-HN5c···O18	0.84(2)	2.43(2)	2.940(3)	120(2)	electrostatic bond
N5-HN5d···O11	0.89(2)	2.22(2)	3.067(2)	159(2)	hydrogen bond
N5-HN5d···O10	0.89(2)	2.32(2)	3.018(3)	136(2)	electrostatic bond

* The NH_4···O bond is interpreted as being predominantly an ordered hydrogen bond if *d*(H···O) is short (< 2.27 Å) and <N–H···O is large (> 140°).

Table 6b. Bond distances and angles for N–H–O bonds in huizingite-(Al).

N–H···O	*d*(N–H)	*d*(H···O)	*d*(N–O)	<N–H···O	NH_4···O bonding*
N1-HN1a···O14	0.86(2)	2.00(2)	2.824(4)	159(3)	hydrogen bond
N1-HN1b···O2	0.90(2)	2.15(2)	3.008(4)	161(3)	hydrogen bond
N1-HN1c···O14	0.91(2)	2.37(3)	3.056(4)	132(3)	electrostatic bond
N1-HN1c···O16	0.91(2)	2.20(2)	3.086(4)	163(3)	hydrogen bond
N1-HN1d···O10	0.88(2)	2.66(3)	3.081(4)	110(2)	electrostatic bond
N1-HN1d···O11	0.88(2)	2.16(2)	2.957(4)	149(3)	hydrogen bond
N2-HN2a···O11	0.87(2)	2.17(2)	3.030(4)	170(3)	hydrogen bond
N2-HN2b···O5	0.88(2)	2.10(3)	2.797(4)	135(3)	hydrogen bond
N2-HN2c···O1	0.87(2)	2.45(3)	2.996(4)	121(3)	electrostatic bond
N2-HN2c···O13	0.87(2)	2.18(3)	2.902(4)	140(3)	hydrogen bond
N2-HN2c···O16	0.87(2)	2.80(3)	3.254(4)	114(3)	electrostatic bond
N2-HN2d···O15	0.93(2)	2.63(3)	3.277(5)	127(3)	electrostatic bond
N2-HN2d···O16	0.93(2)	2.08(2)	2.962(4)	160(3)	hydrogen bond
N3-HN3a···O10	0.89(2)	2.09(2)	2.926(4)	157(3)	hydrogen bond
N3-HN3a···OW2	0.89(2)	2.71(3)	3.251(4)	121(3)	electrostatic bond
N3-HN3b···O13	0.93(2)	1.83(2)	2.729(4)	163(3)	hydrogen bond
N3-HN3c···O9	0.84(2)	2.10(3)	2.836(4)	146(3)	hydrogen bond
N3-HN3c···O15	0.84(2)	2.91(4)	3.258(5)	107(3)	electrostatic bond
N3-HN3d···O3	0.89(2)	2.42(3)	3.163(4)	142(3)	electrostatic bond
N3-HN3d···O6	0.89(2)	2.34(3)	2.860(4)	118(3)	electrostatic bond
N4-HN4a···O14	0.88(2)	1.98(2)	2.847(4)	166(3)	hydrogen bond
N4-HN4a···O15	0.88(2)	2.66(3)	3.092(4)	112(2)	electrostatic bond
N4-HN4b···O5	0.85(2)	2.11(2)	2.860(4)	148(3)	hydrogen bond
N4-HN4b···O2	0.85(2)	2.77(3)	3.100(3)	105(2)	electrostatic bond
N4-HN4c···O6	0.89(2)	2.00(2)	2.883(4)	171(3)	hydrogen bond
N4-HN4c···O9	0.89(2)	2.80(3)	3.103(4)	102(2)	electrostatic bond
N4-HN4d···O1	0.89(2)	2.51(3)	3.122(3)	126(2)	electrostatic bond
N4-HN4d···O4	0.89(2)	2.11(2)	2.999(3)	172(3)	hydrogen bond
N5-HN5a···O6	0.90(3)	2.11(4)	2.979(2)	163(9)	hydrogen bond
N5-HN5b···O1	0.90(3)	1.95(3)	2.837(2)	170(7)	hydrogen bond
N5-HN5c···O9	0.90(3)	1.99(4)	2.872(3)	164(8)	hydrogen bond

* The NH_4···O bond is interpreted as being predominantly an ordered hydrogen bond if *d*(H···O) is short (< 2.27 Å) and <N–H···O is large (> 140°).

982 Table 7a. Bond-valence analysis for carlsonite. Values are expressed in valence units.*

	O1	O2	O3	O4	O5	O6	O7	O8	O9	O10	O11	O12	O13	O14	O15	O16	O17	O18	O19	O20	O21	O22	O23	O24	O25	OW1	OW2	OW3	OW4	OW5	OW6	OW7	Σ_c
$NH_4$1					0.20 0.08				0.16	0.18											0.17		0.04								0.05		0.68
$NH_4$2	0.13	0.21											0.19	0.15			0.19	0.11															0.98
$NH_4$3	0.10												0.14				0.14 0.06		0.11										0.08	0.16		0.12	0.61
$NH_4$4						0.15			0.18			0.05									0.14 0.11	0.08								0.19		0.70
$NH_4$5	0.15					0.13		0.07		0.12	0.10			0.16				0.15						0.09									0.67
Fe1			0.49				0.51				0.51									0.53					0.66	0.40							3.10
Fe2								0.53								0.52			0.49				0.47		0.65		0.43						3.09
Fe3				0.55								0.47			0.49									0.52	0.60			0.45					3.08
S1	1.60	1.59	1.42	1.40																													6.01
S2					1.62	1.58	1.46	1.42																									6.08
S3									1.61	1.54	1.42	1.42																					5.99
S4													1.61	1.54	1.43	1.43																	6.01
S5																	1.64	1.60	1.46	1.44													6.14
S6																					1.58	1.58	1.44	1.40									6.00
HW1a																						0.19				0.81							1.00
HW1b														0.20												0.80							1.00
HW2a																											0.80		0.20				1.00
HW2b										0.20																	0.80						1.00
HW3a																												0.80	0.20				1.00
HW3b						0.21																						0.79					1.00
HW4a																													0.80			0.20	1.00
HW4b																										0.14			0.86				1.00
HW5a																														1.00			1.00
HW5b		0.14																												0.86			1.00
HW6a																															1.00		1.00
HW6b																															1.00		1.00
HW7a																		0.18														0.82	1.00
HW7b		0.11																														0.89	1.00
Σ_a	1.98	2.05	1.91	1.95	1.90	2.07	1.97	2.02	1.95	2.04	2.03	1.94	1.94	2.05	1.92	1.95	2.03	2.04	2.06	1.97	2.00	1.85	1.95	2.01	1.91	2.15	2.03	2.04	2.14	2.02	2.24	2.03	

983 *NH_4^+–O bond strengths from Garcia-Rodriguez *et al*. (2000); Fe^{3+}–O bond strengths from Brown and Altermatt (1985); Si^{4+}–O bond strengths
984 from Brese and O'Keeffe (1991).
985
986

987 Table 7b. Bond-valence analysis for huizingite-(Al). Values are expressed in valence units.*

	O1	O2	O3	O4	O5	O6	O7	O8	O9	O10	O11	O12	O13	O14	O15	O16	OH	OW1	OW2	Σ_c
$NH_4$1		0.12								0.10	0.14	0.06		0.20 0.11		0.10				0.83
$NH_4$2	0.12				0.21						0.11		0.16		0.06	0.06 0.14				0.86
$NH_4$3			0.08			0.18			0.19	0.15			0.26		0.06					0.92
$NH_4$4	0.09	0.09		0.12	0.18	0.17			0.09					0.19	0.10					1.03
$NH_4$5	0.19 ×2→					0.13 ×2→			0.17 ×2→											0.98
Al1			0.40 ×2→				0.55 ×2→										0.55 ×2→			2.99
Al2				0.49				0.49				0.49					0.55	0.49	0.50	3.01
S1	1.58	1.57	1.44	1.42																6.01
S2					1.64	1.60	1.44	1.43												6.11
S3									1.58	1.55	1.50	1.42								6.05
S4													1.60	1.55	1.55	1.51				6.21
H1											0.18						0.82			1.00
HW1a																0.22		0.78		1.00
HW1b		0.19																0.81		1.00
HW2a										0.21									0.79	1.00
HW2b															0.24				0.76	1.00
Σ_a	1.98	1.97	1.92	2.03	2.03	2.08	1.99	1.92	2.03	2.01	1.93	1.97	2.02	2.05	2.01	2.03	1.92	2.08	2.05	

988 *NH_4^+–O bond-valence parameters from Garcia-Rodriguez *et al*. (2000); all other bond-valence parameters from Brown and Altermatt (1985).
989 The Al1–O and Al2–O bond strengths are based upon the refined Al/Fe site occupancies.
990

Fig.1

Fig.2

Fig.3

Fig.4

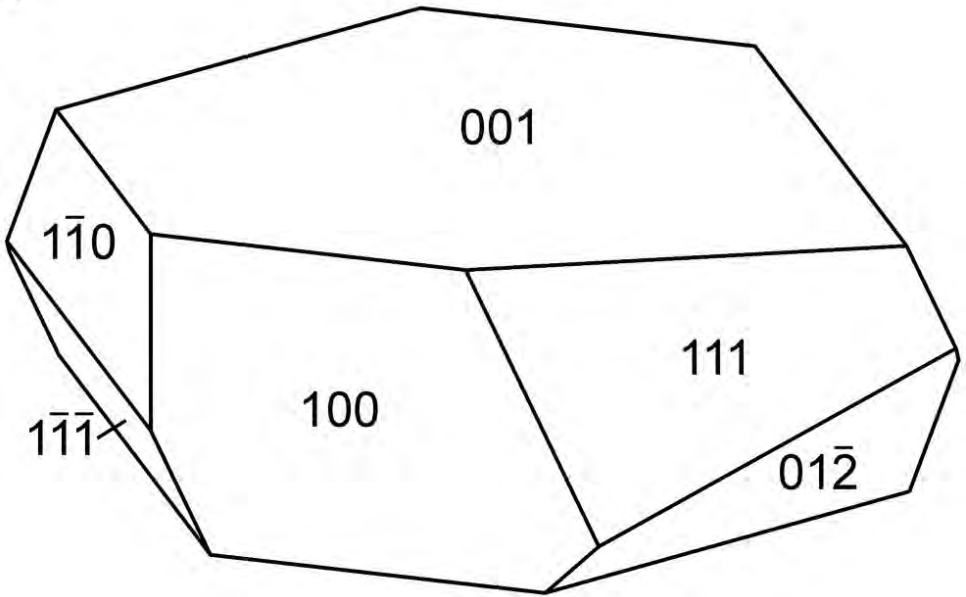

Fig.5

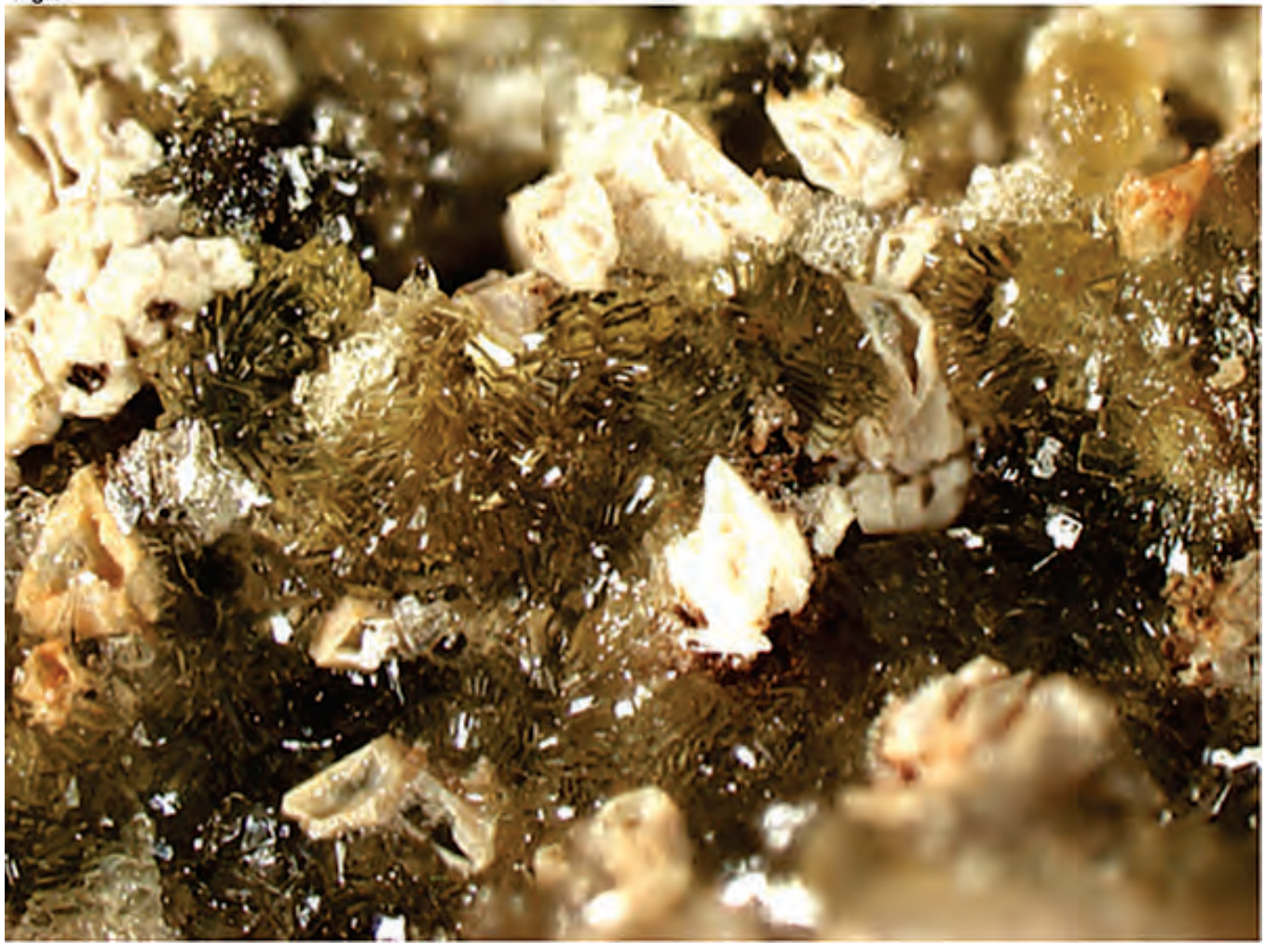

Fig.6

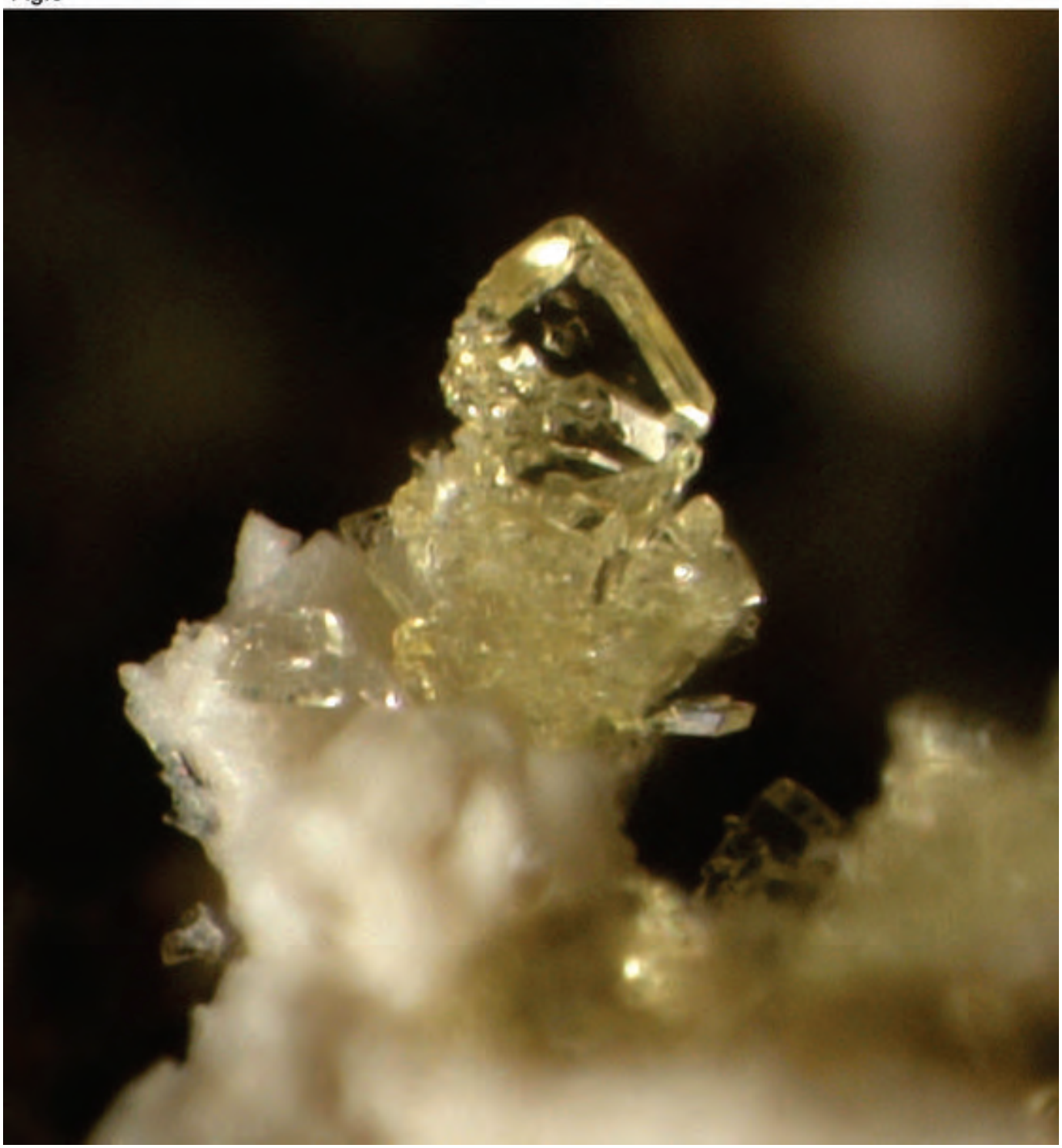

Fig.7

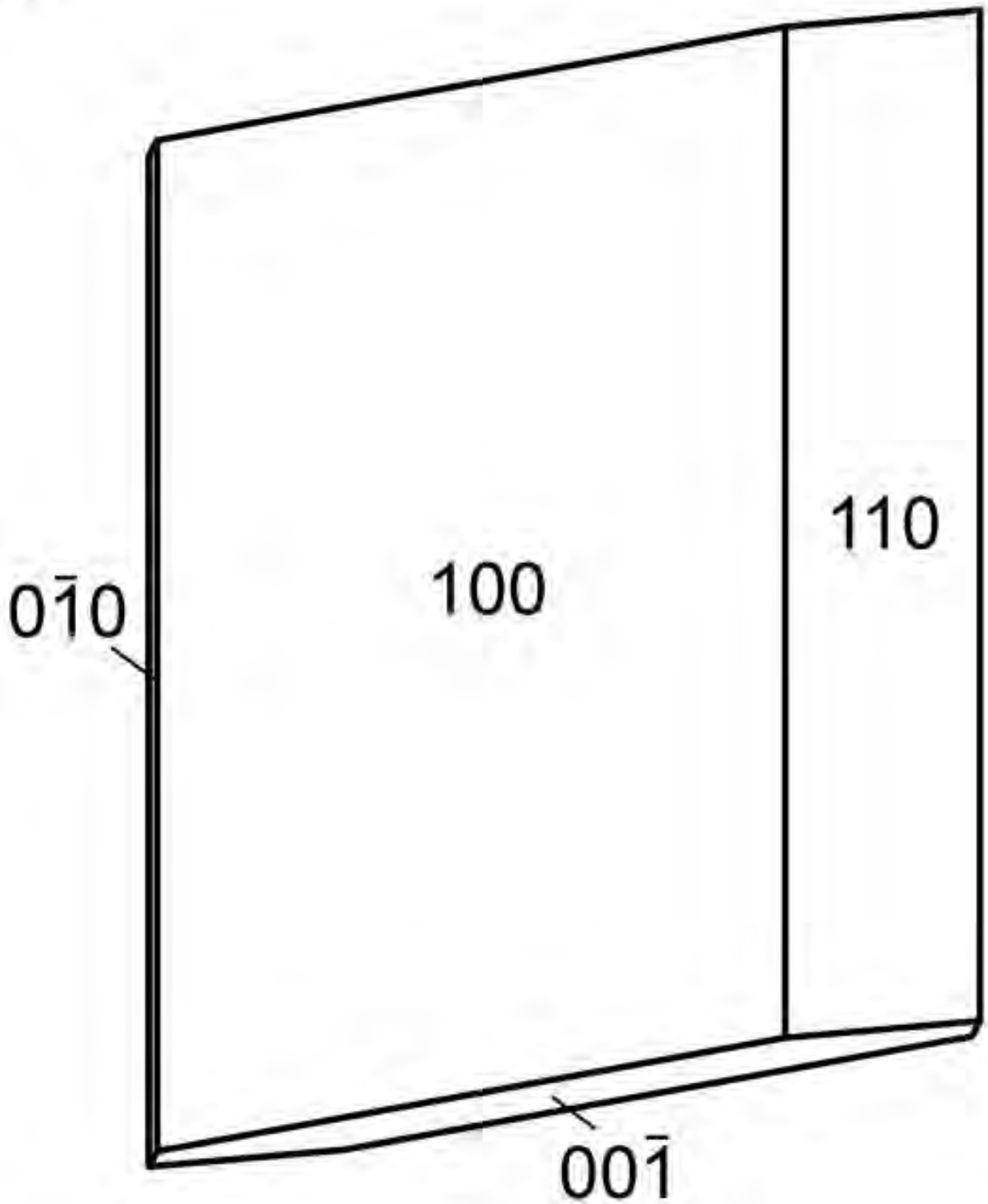

Figure 8

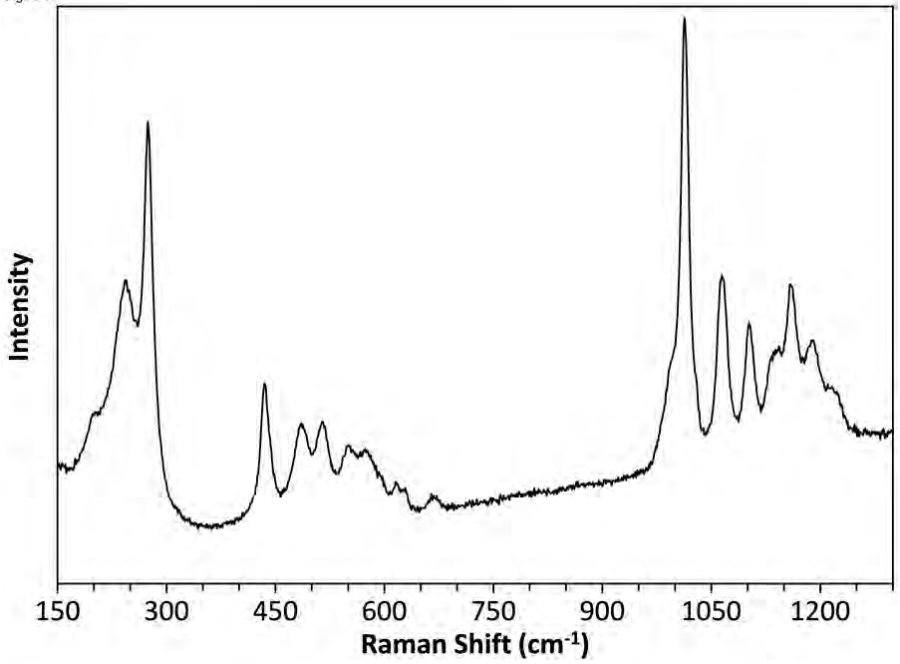

Figure 9

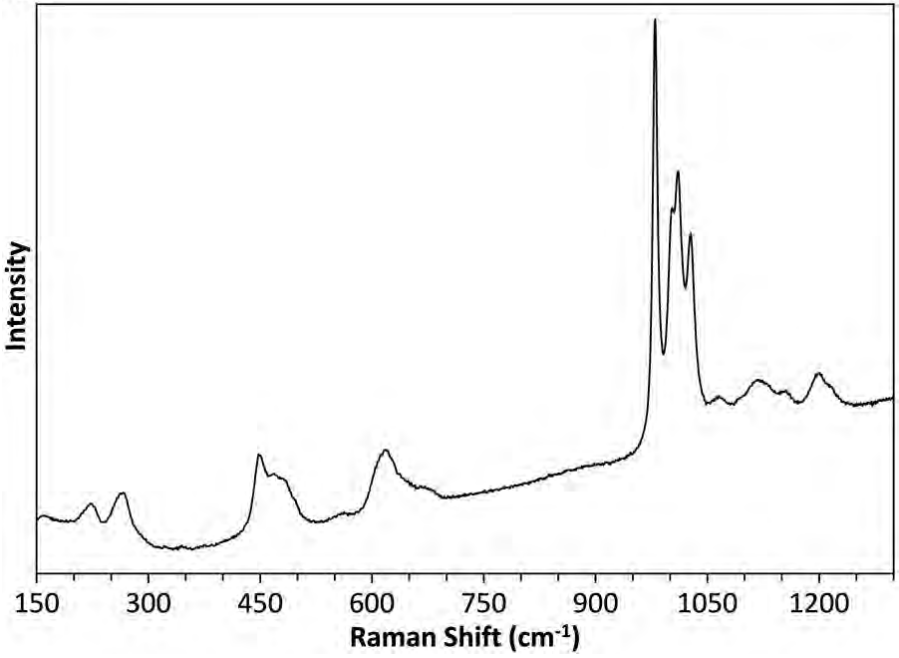

Figure 10

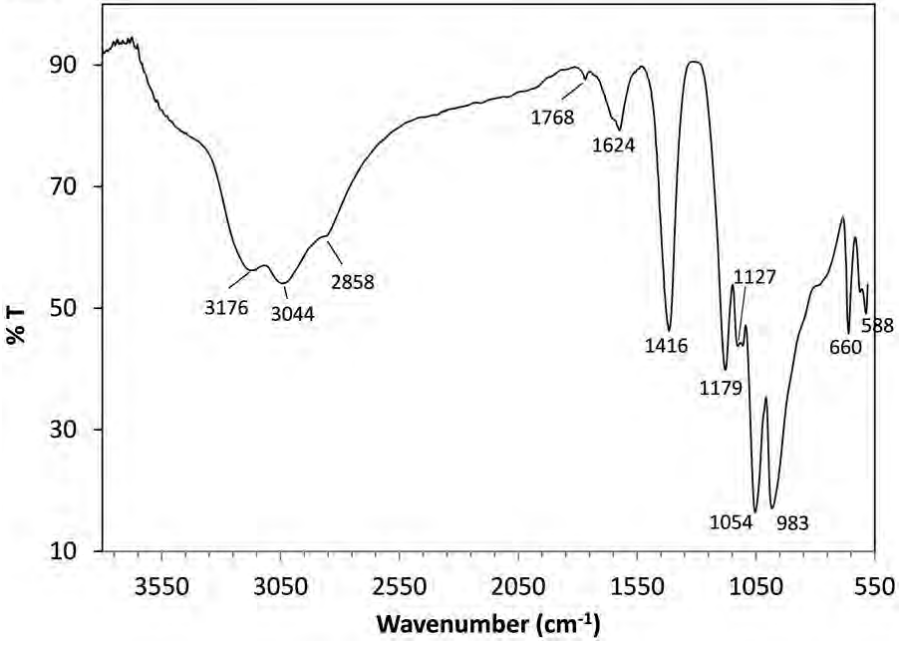
90
70
50
30
10
% T
3550
3050
2550
2050
1550
1050
550
Wavenumber (cm-1)
3176
3044
2858
1768
1624
1416
1179
1127
1054
983
660
588

Figure 11

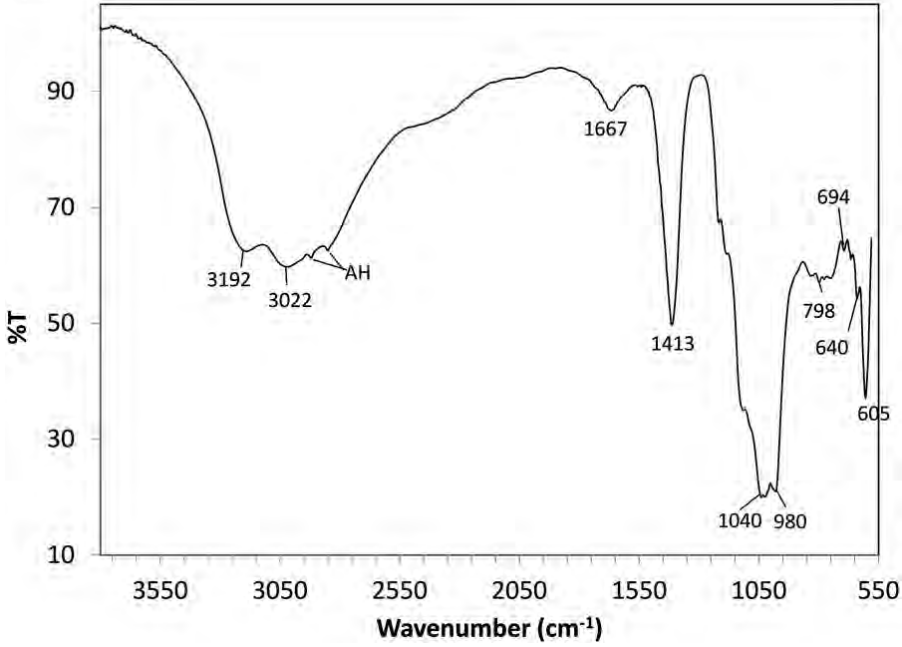
90
70
50
30
10
%T
3550
3050
2550
2050
1550
1050
550
Wavenumber (cm-1)
3192
3022
AH
1667
1413
1040
980
694
798
640
605

Fig.12

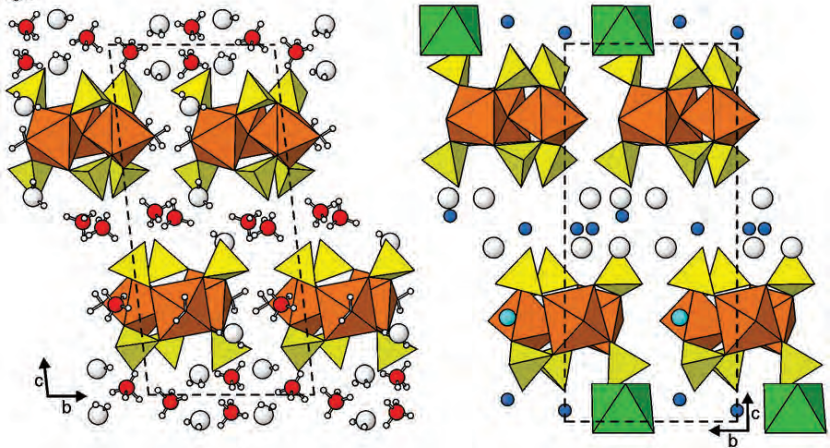

Fig.13

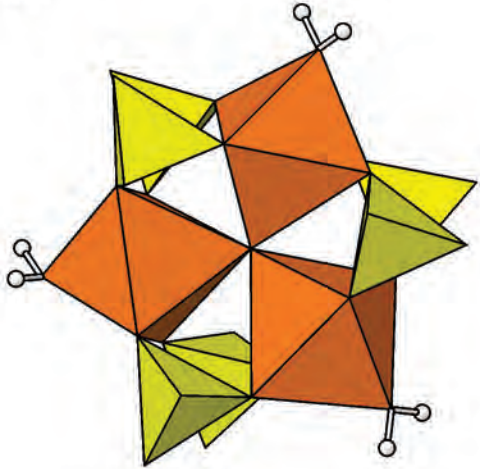

carlsonite

$[Fe^{3+}{}_3O(H_2O)_3(SO_4)_6]^{5-}$

cluster

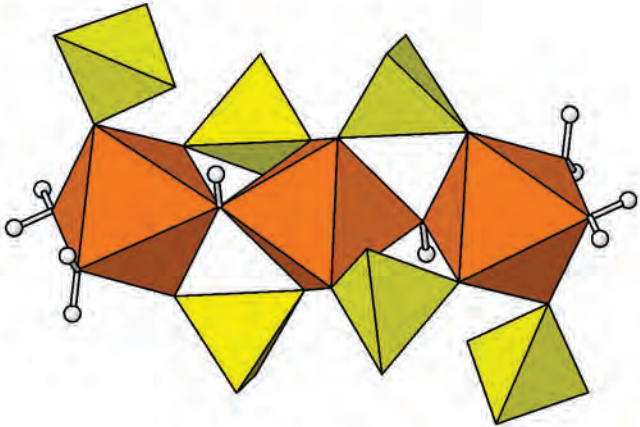

huizingite

$[(Al,Fe^{3+})_3(OH)_2(H_2O)_4(SO_4)_6]^{5-}$

cluster

Fig. 14